Degenerate scales for thin elastic plates with Dirichlet boundary conditions

Alain Corfdir, Guy Bonnet

Degenerate scales for thin elastic plates with Dirichlet boundary conditions

Alain Corfdir. Guy Bonnet

Abstract A degenerate scale occurs when a loss of uniqueness of the solution of the boundary integral equations happens for that scale of the problem. We consider here the biharmonic 2D problem with Dirichlet boundary conditions which models the bending behavior of a clamped isotropic Kirchhoff plate. We extend several results about degenerate scales previously found for the Laplace and Lamé equation to the biharmonic equation in 2 dimensions. The degenerate scales are obtained from a 4×4 discriminant matrix whose shape is provided for different kinds of domain symmetry. We show that degenerate scales can be obtained from a minimization problem. Then, we compare the degenerate scales of two boundaries, one included within the other. For smooth star-shaped curves, we show that there are only two degenerate scales, give sufficient conditions for not being at a degenerate scale and produce bounds to the degenerate scales. For symmetric smooth simply connected curves there are also only two degenerate scales. For these symmetric cases, the use of complex variables allows us to go further and to link the problem of biharmonic equation to the one of plane elasticity and to give information, including bounds and exact values of degenerate scales, for many cases, while until now only very few ones were known. Our results have some consequences for the biharmonic outer radius defined by Pólya and Szegö. The numerical computation of degenerate scales by using boundary elements confirms the theoretical results.

1 Introduction

There is a long history of the mathematical study of the bending of thin elastic plates since the pioneering work of Sophie Germain at the beginning of the nineteenth century. For thin isotropic bending plates (Kirchhoff plates), the transversal displacement u satisfies the biharmonic equation $\Delta^2(u) = 0$. This is also the case for stratified plates made of homogeneous isotropic materials. Selvadurai [50] stated that "the exact first usage of the biharmonic equation is not entirely clear". However, a review of the biharmonic equation, its history and its application to Mechanics can be found in his book. A large review has also been given in Ref. [36]. For the literature from the beginning of the last century, one can cite the early works of Lauricella [34] and Hadamard [23]. Later on, the use of complex boundary integrals to solve boundary value problems on plates has been introduced in Refs. [41,42,44] by Muskhelishvili using the Goursat decomposition [22] of a biharmonic function u: $u = \Re\{\bar{z} f(z) + g(z)\}$, where f and g are two harmonic functions. Concerning the use of this

A. Corfdir (✉)
Laboratoire Navier, École nationale des ponts et chaussées, UMR 8205 CNRS, Université Gustave Eiffel, Champs-sur-Marne, France
E-mail: alain.corfdir@enpc.fr

G. Bonnet
Laboratoire Modélisation et Simulation Multi-Echelle, UMR 8208 CNRS, Université Gustave Eiffel, 5 Boulevard Descartes, 77454 Marne la Vallée Cedex, France
E-mail: guy.bonnet@u-pem.fr

boundary integral equations for biharmonic problem, one can cite the pioneering works of Jaswon [31,32], using a real version of the Goursat decomposition.

The book of Hsiao and Wendland [30] provides a modern mathematical approach to the use of boundary integral equations to solve biharmonic boundary value problems. Theories taking into account also shear strains were developed by Mindlin [38] and Reissner [48] and taken up by different authors like [12]; the important case of laminated plates has been investigated [47,49, e.g.] and the development of refined theories has been continued [1,52, e.g.]. The paper of Meleshko and Selvadurai [35] presents the role of the biharmonic equation in different mechanical problems and introduces several contributions dealing for example with the variable thickness plates or functionally graded materials. In the following literature examination, we focus on the specific problem of degenerate scales for the biharmonic problem/Kirchhoff's thin plate theory.

1.1 The biharmonic equation

The biharmonic operator can be written as

$$\Delta^2(u) = \frac{\partial^4 u}{\partial x_1^4} + 2\frac{\partial^4 u}{\partial x_1^2 \partial x_2^2} + \frac{\partial^4 u}{\partial x_2^4}. \tag{1}$$

One of the main application of the biharmonic equation is related to the study of thin plates, where u is the transversal displacement of the plate, but this equation is also useful in fluid mechanics for studying the slow flow of viscous fluids.

1.2 Boundary conditions

A boundary value problem related to the biharmonic equation has a solution if suitable boundary conditions at the boundary Γ of a domain Ω are defined. These boundary conditions involve the data of 2 scalar functions at each boundary point. Focusing on the application to thin plates, these scalar functions can be: the values of u, the normal derivative of u at the boundary, or the values of the bending moment $M(u)$ or shear force $N(u)$ defined by

$$M(u) = \nu\Delta u + (1-\nu)\left(\frac{\partial^2 u}{\partial x_1^2}n_1^2 + 2\frac{\partial^2 u}{\partial x_1 \partial x_2}n_1 n_2 + \frac{\partial^2 u}{\partial x_2^2}n_2^2\right), \tag{2}$$

$$N(u) = -\frac{\partial \Delta u}{\partial n} + (1-\nu)\frac{d}{ds}\left(\left(\frac{\partial^2 u}{\partial x_1^2} - \frac{\partial^2 u}{\partial x_2^2}\right)n_1 n_2 - 2\frac{\partial^2 u}{\partial x_1 \partial x_2}\left(n_1^2 - n_2^2\right)\right), \tag{3}$$

where n_1, n_2 are the components of the normal to the boundary and $\frac{\mathrm{d}}{\mathrm{d}s}$ is the tangent derivative. ν is the Poisson's ratio. We follow the notation of [28], despite the common use in engineering of V for the shear force. Some authors have a different convention of sign for N (see e.g. [6]).

The Poisson's ratio in 3D elasticity is comprised between 0 and 0.5 except for very specific cases where the Poisson's ratio can become negative. In the case of plane stresses, the range of Poisson's ratio can be extended to the range [0, 1]. Following [30], we name "Dirichlet boundary condition" the problem where both the displacement and the rotation are given on the whole boundary. As for Neumann boundary condition, it is defined by imposing the values of $M(u)$, $N(u)$ on the boundary Γ. This naming is consistent with the usual ones in elasticity: Dirichlet conditions are related to kinematic boundary conditions and Neumann condition is related to the efforts applied at the boundary (like the traction in elasticity).

Of course, some "Robin type" conditions are also possible: $u - kN = 0$; $\partial u/\partial n - k'M = 0$. Even more general boundary conditions can be considered [33]. The special case with $u = 0$ and $\partial u/\partial n = 0$ is the clamped plate case.

From a general point of view, it is important to distinguish the uniqueness of solution of the Boundary Value Problem (i.e. the problem of degenerate scales) from the loss of uniqueness of the boundary integral equation, that appears at some specific scales, i.e. degenerate scales.

The interior boundary value problem has a unique solution for the Dirichlet condition and the Neumann condition (see for example [30, Theorem 2.4.1]).

For the exterior problems, it is necessary to add an extra radiation condition at infinity to ensure the uniqueness. The interior mixed problem (u given on the whole boundary Γ and M given on Γ_1 and N given on Γ_2 with $\Gamma = \Gamma_1 \cup \Gamma_2$) has also a unique solution [3].

1.3 Boundary integral equations

A boundary integral formulation of the boundary value problem (BVP) with physical (real) quantities was given in [2]. An early comparison of different methods can be found in [20].

Some authors introduce an auxiliary function $\Delta u = w$ to write a system of two BIEs (boundary integral equations) [21,39]. This is appropriate for the case of a simply supported plate [25].

There are 4 boundary integral equations which can been deduced from the Calderón's projector, see for example [29,30] (plates) and [4] (beams). They are defined in Appendix A. Naming these boundary integral equations from (1) to (4), the first Eq. (1) is the limit of the representation formula and the other equations are obtained by applying different boundary operators of increasing order.

The possible loss of uniqueness of integral equations for some scales of the problem has been noticed by different authors including [10,18]. The related scales where this loss of uniqueness occurs are called "degenerate scales". If the problem is at such a scale, the boundary integral equation has a non-null solution for homogeneous boundary conditions and has an infinity of solutions for non-null boundary conditions. As a consequence, the discretized system obtained by a Boundary Element discretization becomes singular.

For solving a boundary value problem, one must retain 2 equations out of 4. It means $\binom{4}{2} = 6$ possible combinations. Only the groups (1, 2) and (3, 4) are considered in the summarizing table of [30] for the Dirichlet and Neumann problems. The paper [6] considers the 6 combinations for the special case of a circular plate. The degenerate scales may be found, depending on the chosen combination; the combination (3, 4) is the only one with no degenerate scale. We will focus this study on the group (1, 2).

Writing the boundary integral equation related to the bilaplacian is effected by using a fundamental solution (Green function) related to the differential operator. The usual fundamental solution is $\frac{1}{8\pi} r^2 \ln(r)$. However, other choices are possible, as $\frac{1}{8\pi} r^2 \ln(\mu r)$, $r^2(\ln(r) - 1)$ and $\frac{1}{8\pi} r^2 \ln(r) + c$ that were considered in [5,9,13,51] respectively. From a general point of view, the degenerate scales depend on the choice of the fundamental solution [5,9]. This paper is restrained to the previously described usual fundamental solution.

1.4 Previous results on degenerate scales related to the biharmonic equation

Using a system of augmented boundary integrals, Costabel and Dauge [18] searched for a means to characterize if a domain is at a degenerate scale for the biharmonic equation. They built a fourth-order symmetric "discriminant matrix" $\mathbf{B}_\Gamma$ such that the boundary integrals are at a degenerate scale if and only if this matrix is singular.

In [18], it is proved that there are at least 2 degenerate scales. In [19], it is stated that there are between 1 and 4 degenerate scales.

Studying the eigenvalues of the discriminant matrix makes it possible to show that there are 2 or 4 degenerate scales counting their multiplicities. This is confirmed by the numerical results obtained in Refs. [5,19].

There are only a few cases for which the exact degenerate scales are known. The most important is the one of the circle: the degenerate scale of a circle with Dirichlet boundary condition is $\frac{1}{e}$ with multiplicity 2 for integral equation (1, 2) [20]. It has been proved that the radius leading to a degenerate scale for the interior problem of a circle does not depend on the boundary conditions (excepted for Neumann boundary conditions that have no degenerate scale) but depends on the choice of formulation [6]. The closed form of the degenerate scales is also known for a segment and for the set of the vertices of a parallelogram (Dirichlet boundary condition and formulation (1, 2)) [18].

Different authors developed numerical methods to find the degenerate scales for biharmonic equation. In Refs. [18,19], a numerical method is based on the numerical resolution of an augmented system of 2 boundary integral equations. It provides a 4×4 discriminant matrix from which the degenerate scales can be obtained. Later a method using the singular values has been developed in Ref. [11]. In Ref. [5], it is shown that the number of degenerate scales depends on the fundamental solution used; in this paper, the degenerate scales are calculated for a circle, an ellipse with the major semi-axis equal to twice the minor semi-axis and a triangle (30°, 60°, 90°).

1.5 The scope of the present paper

This paper focuses on the Dirichlet boundary condition, for smooth boundaries using the most usual boundary integral system (1, 2). Its main achievements include new results on the number of the degenerate scales by combining a new monotonicity property with the previous results of Ref. [18] and the calculation of degenerate scales by using a complex representation of the solution of biharmonic equation in the case of domains having given symmetries.

In Sect. 2, we consider the degenerate scales of the interior problem of a multi-connected domain.

In Sect. 3, we recall the construction of a system of augmented BIEs which led [18] to define a discriminant matrix $\mathbf{\Lambda}$ that is singular if and only if the problem is at a degenerate scale. This matrix can be found also by the study of an exterior boundary value problem with a specific radiation condition or by a minimizing problem of integral on the boundary. This approach generalizes a method used in Ref. [26] for Laplace equation and in Ref. [16] for Lamé equation.

In Sect. 4, we consider the case of two boundaries one being included in the other and show that $\mathbf{\Lambda}$ have a monotonic feature for two domains, one within another. For star shaped curves, it is then possible to conclude that there are only two degenerate scales.

In Sect. 5, we first consider the consequence of symmetries of boundary symmetries on the matrix $\mathbf{\Lambda}$, in the spirit of Ref. [18]. Then for these symmetrical cases, complex variable methods allow us to connect degenerate scales for the biharmonic equation to those for plane elasticity. This allows us to find exact solutions for a large type of boundaries and to give some bounds for plate degenerate scales.

Section 6 discusses the notion of the biharmonic outer radius as defined in Ref. [46].

Section 7 deals with the computation of degenerate scales by boundary elements. It gives numerical examples for both simply connected and multi connected boundaries.

The conclusion (Sect. 8) summarizes the main results.

2 Degenerate scales of the interior problem of a multi-connected domain

In a first step, we recall shortly the argument showing that the interior Dirichlet boundary problem has a unique solution. Next, we present the boundary integral equations for the Dirichlet problem and display relations between the degenerate scales related to different domains.

2.1 Uniqueness of the interior Dirichlet boundary value problem

The uniqueness comes from the following Green identity (see for example [30, p. 80] or [40]). The Green's identity is not unique for the biharmonic operator. In order to make apparent the flexure moment and normal force at the boundary, a specific Green's identity is obtained by writing the biharmonic operator in the form

$$\Delta^2(u) = \frac{\partial^2}{\partial x_1^2}\left(\frac{\partial^2 u}{\partial x_1^2} + \nu\frac{\partial^2 u}{\partial x_2^2}\right) + 2(1-\nu)\frac{\partial^2}{\partial x_1 \partial x_2}\frac{\partial^2 u}{\partial x_1 \partial x_2} + \frac{\partial^2}{\partial x_2^2}\left(\nu\frac{\partial^2 u}{\partial x_1^2} + \frac{\partial^2 u}{\partial x_2^2}\right). \tag{4}$$

Introducing $a(u, v)$ defined by

$$a(u, v) = \nu\Delta u\Delta v + (1-\nu)\sum_{i,j=1}^{2}\left(\frac{\partial^2 u}{\partial x_i \partial x_j}\right)\left(\frac{\partial^2 v}{\partial x_i \partial x_j}\right), \tag{5}$$

the Green's identity can be written as

$$\int_\Omega u(\Delta^2 v) = 0 = \int_\Omega a(u, v) - \int_\Gamma \left[\frac{\partial u}{\partial n}M(v) + uN(v)\right]. \tag{6}$$

If we consider that $u = u_1 - u_2$ is the difference between two solutions of the problem with the same Dirichlet boundary conditions, then u is a solution of the problem with homogeneous boundary conditions.

From (6) we deduce that:

$$\underbrace{\int_{\Omega} a(u,u)}_{K_1} = \underbrace{\int_{\Gamma} \left[\frac{\partial u}{\partial n} M(u) + uN(u)\right]}_{K_2}. \tag{7}$$

Let us consider the integral K_2. The term $uN(u)(x)$ is null if the boundary condition is D_0 ($u = 0$) or if the boundary condition is N_0 ($N(u) = 0$) and is negative or null if the boundary condition is R_0 ($ku + N(u) = 0; k > 0$). In the same line, we can also conclude that $\frac{\partial u}{\partial n} M(u)(x) \leq 0$. So finally, we get $K_2 \leq 0$.

The bilinear form $a(u,u)$ can be written as $(\frac{\partial^2 u}{\partial x_1^2} + \nu \frac{\partial^2 u}{\partial x_2^2})^2 + (1-\nu^2)(\frac{\partial^2 u}{\partial x_2^2})^2 + 2(1-\nu)(\frac{\partial^2 u}{\partial x_1 \partial x_2})^2$ and is pointwise ≥ 0. So we conclude $K_1 \geq 0$. Comparing with K_2 leads to $K_1 = 0$. Then $u = a_0 + a_1 x_1 + a_2 x_2$ and the Dirichlet boundary conditions ensures that $u = 0$. This leads to the uniqueness of the solution.

2.2 The system of boundary integral equations for Dirichlet boundary condition and the related degenerate scale

We write the system of BIEs following mainly the notations of Ref. [30]:

$$\begin{cases} \displaystyle\int_{\Gamma} (E(x,y)\phi_3(y) + \frac{\partial E}{\partial n_y}\phi_2(y) - M_y(E)(x,y)\phi_1(y) - N_y(E)(x,y)\phi_0(y))\mathrm{d}S_y = \frac{1}{2}\phi_0(x), \\ \displaystyle\int_{\Gamma} \left(\frac{\partial E(x,y)}{\partial n_x}\phi_3(y) + \frac{\partial^2 E(x,y)}{\partial n_x \partial n_y}\phi_2(y) \right. \\ \displaystyle\left. \quad - \frac{\partial M_y(E)(x,y)}{\partial n_x}\phi_1(y) - \frac{\partial N_y(E)(x,y)}{\partial n_x}\phi_0(y) \right) \mathrm{d}S_y = \frac{1}{2}\phi_1(x), \end{cases} \tag{8}$$

with

$$E(x,y) = \frac{1}{8\pi} r^2 \ln(r) \quad \text{with} \quad r = \sqrt{(x_1 - y_1)^2 + (x_2 - y_2)^2}. \tag{9}$$

This formulation is named formulation (u, θ) in Ref. [6] and system of BIEs of the first kind in Ref. [30] and also (1, 2). As recalled in Appendix A, ϕ_3 is the shear force, ϕ_2 the bending moment, ϕ_1 the rotation and ϕ_0 the normal displacement.

In the following, we say that this system of BIEs is at a degenerate scale for Dirichlet boundary conditions if this system has a non-null solution (ϕ_2, ϕ_3) satisfying a homogeneous Dirichlet boundary condition, i.e. $\phi_1 = 0, \phi_2 = 0$.

2.3 An important property of the degenerate scale of a bounded multi-connected domain

In this subsection, we study the case of a bounded multi-connected domain and we provide the following result: the degenerate scale depends on the exterior boundary and not on the possible internal boundaries. More precisely, following the same argument as in Ref. [54] for plane elasticity, we show in the following that the degenerate scales of the interior problem related to the boundary Γ_0 are degenerate scales of the problems with holes with a boundary $\Gamma = \Gamma_0 \cup \Gamma_1 \cdots \cup \Gamma_n$, where $\Gamma_i, i \neq 0$ are the boundaries of the holes inside Γ_0 (Fig. 1).

We still consider the case of the Dirichlet problem. If there is a non-null solution of the BIEs on the outer boundary Γ_0, then the corresponding representation formula gives a null solution in Ω_0, the interior of Γ_0. Then the BIEs for Ω are satisfied with $(u = 0, \frac{\partial u}{\partial n} = 0, M(u) = 0, N(u) = 0)$ for $x \in \Gamma_i, i \neq 0$ and the problem on Γ is at a degenerate scale.

To prove the reciprocal, we can no longer use the argument of Ref. [54] based on the number of the degenerate scales since we do not know whether the boundaries Γ and Γ_0 have the same number of degenerate scales or not.

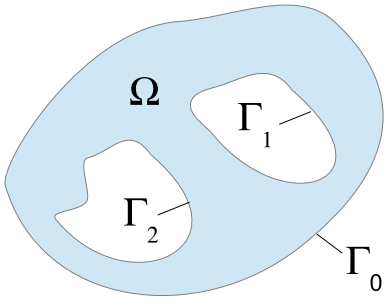

Fig. 1 Bounded multiconnected domain

We assume now that the problem on Γ is at a degenerate scale. Then the representation formula is null in Ω and the corresponding function can be extended to Ω_0. The representation formula v reduces to a single layer potential and then the jumps of v, $\frac{\partial v}{\partial n}$ are null (see for example [17]). Then v is a biharmonic function with homogeneous Dirichlet boundary conditions in the domain bounded by $\Gamma_i, i \neq 0$, and therefore v is null in this domain. Then the jump of $-N(u)$, $M(u)$ on Γ_i is equal to $-\phi_3$, $-\phi_2$ and is null since $u = 0$. We deduce that $w = \int_{\Gamma_0} \phi_3(y)E(x, y) + \phi_2(y)\frac{\partial E}{\partial n_y} = 0$. And finally the boundary Γ_0 is at a degenerate scale. This result is consistent with an early paper [39], which already concludes by using two numerical examples that only the outer boundary determines the degenerate scale for the formulation used by Fuglede [21]. This extends a property which is already known for Laplace equation Eq. [24] and plane elasticity [54] (see also Ref. [8] for a different proof in the case of a circle).

2.4 Influence of the Poisson's ratio ν on the degenerate scales

It should be noted that the degenerate scales do not depend on the parameter ν for the Dirichlet problem. That is clearly different from plane elasticity.

The exterior Dirichlet problem has the same equations as the interior one, and so the degenerate scales do not depend on ν. For other boundary conditions, as $M(u)$ and $N(u)$ depend on ν, a dependency on ν is expected.

3 Three different ways to provide a discriminant matrix $\mathbf{\Lambda}$ related to a given boundary

The paper [18] has defined a discriminant matrix $\mathbf{B}_\Gamma$ that provides the degenerate scales. The authors built an augmented system of Boundary Integral Equations (BIE) that has a unique solution. From this system, they used different boundary conditions to build a discriminant matrix.

In this section, we build, by three different methods, an alternative discriminant matrix $\mathbf{\Lambda}$ which allows us to find the degenerate scales. The results of 3.1, 3.2 and 3.4 are very similar to those in [18] but with a more elementary approach. The matrix $\mathbf{\Lambda}$ will differ from $\mathbf{B}_\Gamma$ by a multiplicative factor in order to simplify the notations.

3.1 Definition of a discriminant matrix using a system of augmented BIEs

Following here [18], we define (p_0, p_1, p_2, p_3) by:

$$p_0(\phi_3) = \frac{1}{8\pi}\int_\Gamma \phi_3 d\Gamma; \quad p_1(\phi_3, \phi_2) = \frac{1}{8\pi}\int_\Gamma (y_1\phi_3 + n_1\phi_2)d\Gamma,$$
$$p_2(\phi_3, \phi_2) = \frac{1}{8\pi}\int_\Gamma (y_2\phi_3 + n_2\phi_2)d\Gamma; \quad p_3(\phi_3, \phi_2) = \frac{1}{8\pi}\int_\Gamma (|y^2|\phi_3 + 2y\cdot n\phi_2)d\Gamma, \tag{10}$$

with n_i the component of n along y_i. We define also $P(x) = B_0 + B_1x_1 + B_2x_2 + B_3(x_1^2 + x_2^2)$. We use in the following the shorter notations: $\mathbf{A} = (A_1, A_2)$ and $\mathbf{B} = (B_1, B_2)$, where $\mathbf{A}$ and $\mathbf{B}$ are constant two components vectors.

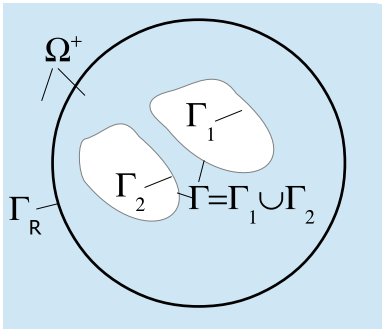

Fig. 2 Exterior domain Ω^+

We now consider the following problem:

$$\begin{cases} \text{Find } (\phi_3, \phi_2) \text{ and } P(x) = B_0 + \mathbf{B}.\mathbf{x} + B_3 r^2 \text{ for given } (A_0, \mathbf{A}, A_3) \text{ such that:} \\ \displaystyle\int_\Gamma E(x,y)\phi_3(y) + \frac{\partial E}{\partial n_y}\phi_2(y) - P(x) = 0, \\ \displaystyle\int_\Gamma \frac{\partial E(x,y)}{\partial n_x}\phi_3(y) + \frac{\partial^2 E(x,y)}{\partial n_x \partial n_y}\phi_2(y) - \frac{\partial P}{\partial n}(x) = 0, \\ A_0 = p_0(\phi_3), \quad A_1 = p_1(\phi_3,\phi_2), \quad A_2 = p_2(\phi_3,\phi_2), \quad A_3 = p_3(\phi_3,\phi_2). \end{cases} \tag{11}$$

This system has a unique solution [18] in terms of $(B_0, \mathbf{B}, B_3)$ for any given values of $(A_0, \mathbf{A}, A_3)$ and the relation between these two vectors is linear. As a consequence, one can consider the matrix $\mathbf{\Lambda}$ that is defined by $(B_0, \mathbf{B}, B_3)^\top = \mathbf{\Lambda}(A_0, \mathbf{A}, A_3)^\top$. We retrieve the problem leading to the matrix $\mathbf{B}_\Gamma$ in [18], up to the $1/8\pi$ factor: $\mathbf{\Lambda} = 8\pi\mathbf{B}_\Gamma$. This problem has a unique solution [18].

From [18] there is a non-null solution of the above problem with $P = 0$ if an only if the matrix $\mathbf{\Lambda}$ (or equivalently $\mathbf{B}_\Gamma$) is singular [18].

From the solution of (11), we define the function u given by the representation formula:

$$u(x) = \int_\Gamma \left(E\phi_3 + \frac{\partial E}{\partial n}\phi_2 \right) \mathrm{d}S_y - B_0 - B_1 x_1 - B_2 x_2 - B_3\, r^2. \tag{12}$$

3.2 Obtention of the discriminant matrix from an exterior boundary value problem

Now, we consider an exterior problem, following the ideas of [27] for Laplace equation, later applied to Lamé's Eq. [16]. The domain that is exterior to the bounded boundary Γ is denoted by Ω^+ (Fig. 2).

This exterior problem is defined by

$$\begin{cases} \Delta^2 u(x) = 0 \; x \in \Omega^+, \\ \text{u satisfies the Dirichlet boundary conditions on } \Gamma, \\ u(x) = A_0 r^2 \ln(r) - \mathbf{A}\cdot\mathbf{x}(2\ln(r)+1) + A_3(\ln(r)+1) \\ \quad - B_0 - \mathbf{B}\cdot\mathbf{x} - B_3 r^2 + c_1\cos(2\theta) + c_2\sin(2\theta) + O(1/r) \\ \text{for given } (A_0, \mathbf{A}, A_3) \text{ and } r \to \infty. \end{cases} \tag{13}$$

We assume that u is a solution of (13), where c_i and B_i are constant. We intend to show that the solution of this exterior problem allows us to recover the solution of (11) and is the same as the one of (12).

In a first step, we show that A_i and c_i do not appear explicitly in the integral representation of u within Ω^+.

We can apply the Green formula on the domain Ω_R bounded by Γ and the circle Γ_R.

$$\int_{\Omega_R} (\Delta^2(E)u - E\Delta^2(u))\, \mathrm{d}S_y = u(x)$$

$$= \int_{\Gamma \cup \Gamma_R} -N(E)u - M(E)\frac{\partial u}{\partial n} + \frac{\partial E}{\partial n} M(u) + EN(u). \tag{14}$$

It is shown in "Appendix B" that:

$$\begin{aligned} &\int_{\Gamma_R} (-N(E)u - M(E)\frac{\partial u}{\partial n} + \frac{\partial E}{\partial n} M(u) + EN(u)) \mathrm{d}S_y \\ &= -B_0 - \mathbf{B} \cdot x - B_3 r^2. \end{aligned} \tag{15}$$

Then, using the Dirichlet condition on Γ, we conclude to the following representation formula for $x \in \Omega^+$:

$$u(x) = \int_\Gamma \left(\frac{\partial E}{\partial n} M(u) + EN(u) \right) \mathrm{d}S_y - B_0 - \mathbf{B} \cdot x - B_3 r^2. \tag{16}$$

This formula is analogous to the formula (7) of [27] for Laplace equation. It is noticeable that the terms involving $(A_0, \mathbf{A}, A_3, c_1, c_2)$ do not appear in the previous formula.

Next, we define:

$$\phi_2(x) = M(u)(x); \phi_3(x) = N(u)(x), \quad x \in \Gamma, \tag{17}$$

and using the boundary conditions, we can write the 2 BIEs with a source term as defined in problem (14). Taking into account the Dirichlet condition, we have:

$$\begin{aligned} 0 &= \int_\Gamma (E(x, y)\phi_3(y) + \frac{\partial E}{\partial n_y}\phi_2(y)) \mathrm{d}S_y - P(x), \\ 0 &= \int_\Gamma \left(\frac{\partial E(x, y)}{\partial n_x}\phi_3(y) + \frac{\partial^2 E(x, y)}{\partial n_x \partial n_y}\phi_2(y) \right) \mathrm{d}S_y - \frac{\partial P}{\partial n}(x). \end{aligned} \tag{18}$$

We intend now to show that, taking into account the asymptotic behaviour of (16), we recover the augmented boundary value problem of (14).

We must therefore evaluate the terms $(A_0, \mathbf{A}, A_3)$ as functions of (ϕ_2, ϕ_3). For that, it is necessary to evaluate the asymptotic behaviour of $\int_\Gamma E(x, y)\phi_3(y) + \frac{\partial E}{\partial n_y}\phi_2(y)$ when $|x| \to \infty$.

We have the following results:

$$\begin{aligned} E(x, y) &= \frac{1}{8\pi} \left[|x|^2 \ln |x| - x \cdot y(2 \ln |x| + 1) + |y|^2 (\ln(|x| + 1)) \right] \\ &\quad + \alpha_1 \cos(2\theta) + \alpha_2 \sin(2\theta) + O\left(\frac{1}{|x|} \right), \end{aligned} \tag{19}$$

$$\begin{aligned} \frac{\partial E}{\partial n}(x, y) &= \frac{1}{8\pi} \left[-n \cdot x(2 \ln |x| + 1) + 2n \cdot y(\ln |x| + 1) \right] \\ &\quad + \beta_1 \cos(2\theta) + \beta_2 \sin(2\theta) + O\left(\frac{1}{|x|} \right), \end{aligned} \tag{20}$$

with n the outwards normal of Γ at the point x. Then we get the asymptotic behaviour of $u(x)$ when $|x| \to \infty$:

$$\begin{aligned} u(x) = \frac{1}{8\pi} &[|x|^2 \ln |x| \int_\Gamma \phi_3(y) - (2 \ln |x| + 1)x. \int_\Gamma (y\phi_3 + n\phi_2) \\ &+ (\ln |x| + 1) \int_\Gamma |y^2|\phi_3 + 2y \cdot n\phi_2 \\ &+ c_1 \cos(2\theta) + c_2 \sin(2\theta) - P(x) + O\left(\frac{1}{|x|} \right). \end{aligned} \tag{21}$$

We deduce:

$$A_0 = \frac{1}{8\pi} \int_\Gamma \phi_3; \mathbf{A} = \frac{1}{8\pi} \int_\Gamma y\phi_3 + n\phi_2; \quad A_3 = \frac{1}{8\pi} \int_\Gamma |y^2|\phi_3 + 2y \cdot n\phi_2. \tag{22}$$

So, from a solution of (13), we get a solution of the two boundary integral equations of (11) with the same values of $(A_0, \mathbf{A}, A_3)$. The solution of (11) is unique and then the values of $(B_0, \mathbf{B}, B_3)$ are also the same for the two problems.

If $(A_0, \mathbf{A}, A_3)$ is non-null and $P = 0$, then the boundary integral equations have a non-null solution with homogeneous boundary conditions; the problem is then at a degenerate scale. It shows that matrix $\mathbf{\Lambda}$ is a discriminant matrix leading to the degenerate scales of the Dirichlet problem.

Reciprocally, from the solution of (11), we get a solution of (13) by using the representation formula. We deduce the existence and the uniqueness of the solution of (13) from the existence and uniqueness of the solution of (11). The problems (11) and (13) define the same matrix $\mathbf{\Lambda}$.

It is worthwhile noticing that this new method to provide the discriminant matrix is obtained from the boundary integral equation related to a BVP with conditions at infinity instead of from an augmented boundary integral equation.

This new method to get the discriminant matrix will be useful thereafter to find some features of the discriminant matrix. However, even if this new method is built by using a boundary condition at infinity related to an exterior problem, the consequences on the degenerate scale will be also valid for interior problems.

3.3 Obtention of the discriminant matrix from a minimization problem

As shown in the case of elasticity [14], a link between a discriminant matrix and a minimization problem can be a useful way to obtain inequalities concerning degenerate scales.

We consider the following problem:

$$\begin{cases} \text{For given } (A_0, \mathbf{A}, A_3), \text{ minimize} \\ J(\phi_3, \phi_2) = \displaystyle\int_\Gamma \phi_3(x) \left(\int_\Gamma E(x, y)\phi_3(y) + \frac{\partial E}{\partial n_y}\phi_2(y) \mathrm{d}S_y \right) \mathrm{d}S_x \\ + \displaystyle\int_\Gamma \phi_2(x) \left(\int_\Gamma \frac{\partial E(x, y)}{\partial n_x}\phi_3(y) + \frac{\partial^2 E(x, y)}{\partial n_x \partial n_y}\phi_2(y) \mathrm{d}S_y \right) \mathrm{d}S_x, \\ \text{with } p_0(\phi_3) = A_0,\ p_1(\phi_3, \phi_2) = A_1,\ p_2(\phi_3, \phi_2) = A_2,\ p_3(\phi_3, \phi_2) = A_3. \end{cases} \tag{23}$$

We show that the solution of problem (11) is the same as the solution of problem (23). We assume that $(\phi_3, \phi_2, B_0, B_1, B_2, B_3)$ is the solution for (A_0, A_1, A_2, A_3). We consider $(\delta\phi_3, \delta\phi_2)$ such that $p_i(\delta\phi_3, \delta\phi_2) = 0$. We evaluate $J(\phi_3 + \delta\phi_3, \phi_2 + \delta\phi_2)$:

$$\begin{aligned} & J(\phi_3 + \delta\phi_3, \phi_2 + \delta\phi_2) \\ & J(\phi_3, \phi_2) + J(\delta\phi_3, \delta\phi_2) + 2\int_\Gamma \delta\phi_3(x) \left(\int_\Gamma E(x, y)\phi_3(y) + \frac{\partial E}{\partial n_y}\phi_2(y) \right) \\ & \quad + 2\int_\Gamma \delta\phi_2(x) \left(\int_\Gamma \frac{\partial E}{\partial n_x}\phi_3(y) + \frac{\partial^2 E}{\partial n_x \partial n_y}\phi_2(y) \right). \end{aligned} \tag{24}$$

Using that $\int_\Gamma E(x, y)\phi_3(y) + \frac{\partial E}{\partial n_y}\phi_2(y) = P(x)$, $\int_\Gamma \frac{\partial E}{\partial n_x}\phi_3(y) + \frac{\partial^2 E}{\partial n_x \partial n_y}\phi_2(y) = \frac{\partial P}{\partial n}$, the two integrals of (24) can be written as:

$$\begin{aligned} \int_\Gamma \delta\phi_3 P(x) + \int_\Gamma \delta\phi_2 \frac{\partial P}{\partial n} &= B_0 \int_\Gamma \delta\phi_3 + B_1 \int_\Gamma (\delta\phi_3 x_1 + \delta\phi_2 n_1) \\ &\quad + B_2 \int_\Gamma (\delta\phi_3 x_2 + \delta\phi_2 n_2) + B_3 \int_\Gamma \left(\delta\phi_3 \left(x_1^2 + x_2^2 \right) + \delta\phi_2 x \cdot n \right) \\ &= \sum_{i=0}^{3} B_i\, p_i(\delta\phi_3, \delta\phi_2) = 0. \end{aligned} \tag{25}$$

So finally we get $J(\phi_3 + \delta\phi_3, \phi_2 + \delta\phi_2) = J(\phi_3, \phi_2) + J(\delta\phi_3, \delta\phi_2)$. But we have (from Ref. [18]) $J(\delta\phi_3, \delta\phi_2) > 0$ if $p_i(\delta\phi_3, \delta\phi_2) = 0, i = 0, 1, 2$ and $(\delta\phi_3, \delta\phi_2) \neq 0$.

We therefore conclude that the minimum of J is reached for (ϕ_3, ϕ_2).

We can now evaluate the minimum of J, using the same calculation as (25):

$$\min(J) = \sum_{i=0}^{3} B_i\, p_i(\phi_3, \phi_2) = \sum_{i=0}^{3} A_i B_i = (A_0, A_1, A_2, A_3)\mathbf{\Lambda}(A_0, A_1, A_2, A_3)^T. \tag{26}$$

This proves that the unknown matrix $\mathbf{\Lambda}$ can be obtained from a minimization problem, using the symmetry of $\mathbf{\Lambda}$.

3.4 Scaling properties of the discriminant matrix $\mathbf{\Lambda}$

In this section, we study the transformation of the discriminant matrix when a scaling is applied to the boundary problem. To this aim, we consider a change of unit of length (rather than a change of size). We assume therefore that the unit length is divided by ρ. Then the new value l' of a length characterized by ρl.

As a consequence, the condition at infinity (radiation condition) in the new units becomes:

$$\begin{aligned} u = {} & A'_0 r'^2 \ln(r') - \mathbf{A}' \cdot x' \ln(r') + A'_3(\ln(r') + 1) \\ & - B'_0 - \mathbf{B}' x' - B'_3 r'^2 + C' \cos(2\theta - \phi) + O(1/r)). \end{aligned} \tag{27}$$

Substituting x' by ρx in the previous expression and identifying the different terms of the radiation condition in the original units, we get:

$$\begin{aligned} A'_0\rho^2 &= A_0, & B'_0 - A'_3 \ln(\rho) &= B_0, \\ \mathbf{A}'\rho &= \mathbf{A}, & \mathbf{B}'\rho + 2\mathbf{A}'\rho \ln(\rho) &= \mathbf{B}, \\ A'_3 &= A_3, & B'_3\rho^2 - A_0\rho^2 \ln(\rho) &= B_3. \end{aligned} \tag{28}$$

Then we substitute A_i and B_i by their values as functions of A'_i and B'_i in $(B_0, B_1, B_2, B_3)^T = \mathbf{\Lambda}_{in}(A_0, A_1, A_2, A_3)^T$, where $\Lambda_{\mathbf{in}}$ is the initial value of $\mathbf{\Lambda}$, i.e. $\mathbf{\Lambda}_{in} = \mathbf{\Lambda}$. We get:

$$\begin{pmatrix} 1 & 0 & 0 & 0 \\ 0 & \rho & 0 & 0 \\ 0 & 0 & \rho & 0 \\ 0 & 0 & 0 & \rho^2 \end{pmatrix} \left[\begin{pmatrix} B'_0 \\ B'_1 \\ B'_2 \\ B'_3 \end{pmatrix} - \begin{pmatrix} 0 & 0 & 0 & 1 \\ 0 & -2 & 0 & 0 \\ 0 & 0 & -2 & 0 \\ 1 & 0 & 0 & 0 \end{pmatrix} \begin{pmatrix} A'_0 \\ A'_1 \\ A'_2 \\ A'_3 \end{pmatrix} \right] = \Lambda_1 \begin{pmatrix} \rho^2 & 0 & 0 & 0 \\ 0 & \rho & 0 & 0 \\ 0 & 0 & \rho & 0 \\ 0 & 0 & 0 & 1 \end{pmatrix} \begin{pmatrix} A'_0 \\ A'_1 \\ A'_2 \\ A'_3 \end{pmatrix}. \tag{29}$$

Then, we get, as in [20], the value $\mathbf{\Lambda}_\rho$ of the discriminant matrix after scaling:

$$\mathbf{\Lambda}_\rho = \mathbf{D}_\rho(\mathbf{\Lambda} + \ln(\rho)\Psi)\mathbf{D}_\rho, \tag{30}$$

with Ψ defined by (31).

$$\Psi = \begin{pmatrix} 0 & 0 & 0 & 1 \\ 0 & -2 & 0 & 0 \\ 0 & 0 & -2 & 0 \\ 1 & 0 & 0 & 0 \end{pmatrix} \tag{31}$$

and $\mathbf{D}_\rho$ defined by:

$$\mathbf{D}_\rho = \begin{pmatrix} \rho & 0 & 0 & 0 \\ 0 & 1 & 0 & 0 \\ 0 & 0 & 1 & 0 \\ 0 & 0 & 0 & 1/\rho \end{pmatrix}. \tag{32}$$

The degenerate scales are the values of ρ that make singular the scaled matrix $\mathbf{\Lambda}_\rho$. They are given by:

$$\rho_i = \mathrm{e}^{-\lambda_i}, \tag{33}$$

where λ_i are the eigenvalues of $\Psi^{-1}\mathbf{\Lambda}$.

For each value of ρ_i, the matrix $\mathbf{\Lambda}_{\rho_i}$ is singular.

It is worthwhile noticing that the degenerate scales related to a given boundary do not depend on the choice of an orthonormal basis (O, Ox_1, Ox_2). However, the matrix $\mathbf{\Lambda}$ can be modified.

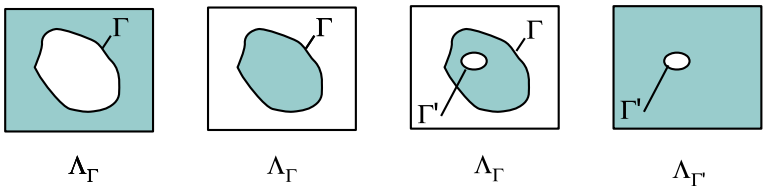

Fig. 3 Boundary included in another one

4 Use of the discriminant matrix to provide some properties of degenerate scales

A first important property is that the discriminant matrix $\mathbf{\Lambda}_\rho$ has 1 negative eigenvalue and 3 positive eigenvalues when $\rho \to 0$, and 3 negative eigenvalues and 1 positive eigenvalue when $\rho \to \infty$. From this result, it can be deduced that there are at least two degenerate scales [18].

In the following, we establish important properties of the discriminant matrix. To this aim, we study in a first step the discriminant matrix of a circle that will be used thereafter as comparison matrix to provide the properties of the discriminant matrix related to other boundaries.

4.1 The discriminant matrix $\mathbf{\Lambda}$ for a circle

In a first step, we look at the matrix $\mathbf{\Lambda}$ for a circle. As it will be seen thereafter, important properties will be obtained by comparison between other domains and circular ones.

We use the solution of the exterior Dirichlet problem with specific behaviour at infinity. We consider that the boundary Γ is a circle of radius R.

Following [18] we define u_1:

$$u_1 = -x_1(2\ln(r) + 1) - B_1 x_1 + \beta \frac{x_1}{r^2}. \tag{34}$$

Using the Dirichlet boundary condition $u_1(R) = 0$, $\frac{\partial u_1}{\partial r}(R) = 0$, we get: $B_1 = -2(\ln(R) + 1)$ and $B_i = 0, i \neq 1$ for $A_0 = 0$, $A_1 = 1$, $A_2 = 0$, $A_3 = 0$. Similarly, we find $B_2 = -(\ln(R) + 1)$ for $A_0 = 0$, $A_1 = 0$, $A_2 = 1$, $A_3 = 0$ and $B_i = 0, i \neq 2$.

We consider also $u_0 = r^2 \ln(r) - B_0 - B_3 r^2$. Using the Dirichlet boundary condition we get: $B_3 = \ln(R) + 1/2$ and then, $B_0 = -R^2/2$. We consider now $u_3 = (\ln(r) + 1) - B_0 - B_3 r^2$. Following the same way, we find: $B_3 = 1/(2R^2)$, $B_0 = (\ln(R) + 1/2)$

We can now build the $\mathbf{\Lambda}$ matrix:

$$\mathbf{\Lambda} = \begin{pmatrix} -\frac{R^2}{2} & 0 & 0 & \ln(R) + \frac{1}{2} \\ 0 & -2(\ln(R) + 1) & 0 & 0 \\ 0 & 0 & -2(\ln(R) + 1) & 0 \\ \ln(R) + \frac{1}{2} & 0 & 0 & \frac{1}{2R^2} \end{pmatrix}. \tag{35}$$

This matrix is symmetric, as expected. We know that the solution of the BIEs is unique if $\mathbf{\Lambda}$ is invertible. We find $\det(\mathbf{\Lambda}) = -4(\ln(R) + 1)^2(1/4 + (\ln(R) + 1/2)^2)$. We retrieve that there is only one (double) degenerate scale $R = 1/e$.

4.2 Inequality between $\mathbf{\Lambda}$ matrices for two boundaries one included in the other

We consider the simply connected boundary Γ containing another boundary denoted by Γ' (Fig. 3).

For given (A_0, A_1, A_2, A_3), there is a unique solution of the augmented BIEs system relative to the boundary Γ. This solution can be expressed by the representation formula:

$$u = \int_\Gamma (\phi_3(y) E(x, y) + \phi_2 \frac{\partial E(x, y)}{\partial n_y} \mathrm{d}S_y - P(x, y) \tag{36}$$

This function u satisfies the homogeneous Dirichlet boundary condition and the biharmonic equation in the domain bounded by Γ and so is null in this domain. The augmented BIEs are satisfied on $\Gamma \cup \Gamma'$ with the same A_i and B_i. We conclude the following equality for the discriminant matrices:

$$\mathbf{\Lambda}_\Gamma = \mathbf{\Lambda}_{\Gamma\cup\Gamma'} \,. \tag{37}$$

This remark completes the result for the degenerate scales obtained in Sect. 2. The problem with internal boundaries and an external boundary is characterized by the same discriminant matrix as the one related only to the external boundary.

We denote now $\phi = (\phi_3, \phi_2)$,

$$V_\Gamma(\phi) = \left(\int_\Gamma E(x,y)\phi_3 + \frac{\partial E}{\partial n_y}\phi_2, \int_\Gamma \frac{\partial E(x,y)}{\partial n_x}\phi_3 + \frac{\partial^2 E}{\partial n_x n_y}\phi_2 \right), \tag{38}$$

and $\langle \phi, \phi' \rangle_{\Gamma,\Gamma'}$:

$$\langle \phi, \phi' \rangle_{\Gamma,\Gamma'} = \int_\Gamma \phi_3 \int_{\Gamma'} E(x,y)\phi'_3 + \frac{\partial E}{\partial n_y}\phi'_2 + \int_\Gamma \phi_2 \int_{\Gamma'} \frac{\partial E(x,y)}{\partial n_x}\phi'_3 + \frac{\partial^2 E}{\partial n_x n_y}\phi'_2. \tag{39}$$

We follow here the method used in [14,54] for the case of plane elasticity. For any $(A_0, A_1, A_2, A_3) \neq (0,0,0,0)$, we consider (ϕ, P) the solution of the augmented system of BIEs relative to the boundary Γ with $p_i(\phi) = -A_i$. We consider also ϕ' defined on Γ' such that $p'_i(\phi') = A_i$. We define $\tilde{\Gamma} = \Gamma \cup \Gamma'$ and $\tilde{\phi}(x) = \phi(x), x \in \Gamma$; $\tilde{\phi}(x) = \phi'(x), x \in \Gamma'$.

It comes from these definitions that:

$$\langle \tilde{\phi}, \tilde{\phi} \rangle_{\tilde{\Gamma},\tilde{\Gamma}} = \langle \phi, \phi \rangle_{\Gamma,\Gamma} + \langle \phi, \phi' \rangle_{\Gamma,\Gamma'} + \langle \phi', \phi \rangle_{\Gamma',\Gamma} + \langle \phi', \phi' \rangle_{\Gamma',\Gamma'}. \tag{40}$$

We have: $\langle \phi, \phi \rangle_{\Gamma,\Gamma} = A.\Lambda_\Gamma \cdot A$. It appears that $\langle \phi, \phi' \rangle_{\Gamma,\Gamma'} = \langle \phi', \phi \rangle_{\Gamma',\Gamma}$. The representation formula $V_\Gamma(\phi)$ is equal to P in the interior of Γ. Then:

$$\langle \phi', \phi \rangle_{\Gamma',\Gamma} = \int_{\Gamma'} \phi'_3 P + \phi'_2 \frac{\partial P}{\partial n} = \mathbf{A}\mathbf{\Lambda}_\Gamma(-\mathbf{A}). \tag{41}$$

The function $\tilde{\phi}$ is such that $\tilde{p}_i(\tilde{\phi}) = 0, i = 0, 1, 2$. Then we have: $\langle \tilde{\phi}, \tilde{\phi} \rangle_{\tilde{\Gamma},\tilde{\Gamma}} > 0$ if $\tilde{\phi} \neq 0$ [18]. We finally conclude: $\langle \phi', \phi' \rangle_{\Gamma',\Gamma'} - \mathbf{A}\mathbf{\Lambda}_\Gamma\mathbf{A} > 0$. As this is true for all ϕ' such that that $p'_i(\phi') = A_i$, the inequality holds also for the minimum of $\langle \phi', \phi' \rangle_{\Gamma',\Gamma'}$. For given $\mathbf{A}$ we get $\mathbf{A}\mathbf{\Lambda}_{\Gamma'}\mathbf{A} \geq \mathbf{A}\mathbf{\Lambda}_\Gamma\mathbf{A}$. As this is true for all $\mathbf{A}$, and as the matrices $\mathbf{\Lambda}$, $\mathbf{\Lambda}'$ are symmetric, we finally conclude the following result:

If the boundary Γ' is inside Γ, the related discriminant matrices are characterized by the following inequality:

$$\mathbf{\Lambda}_{\Gamma'} \geq \mathbf{\Lambda}_\Gamma \,. \tag{42}$$

This important property of matrix $\mathbf{\Lambda}$ generalizes similar properties obtained in the case of plane elasticity. It can be extended to the case of a boundary containing a non-connected domain.

4.3 Properties of $\mathbf{\Lambda}$ matrix for star-shaped boundaries

We consider now the case of a star-shaped domain (see Fig. 4). The star-shaped domain is such that any boundary point is connected to the "center" O by a straight segment. It should be noted that a non-convex domain may be star-shaped. For such a domain the homothetic domain of ratio $\rho > 1$ of center O, always contains the original domain and for a ratio $\rho < 1$ the transformed domain is included within the original one.

So, applying the preceding results, we see that $\mathbf{\Lambda}_\rho$ is a decreasing function of the ratio ρ and its eigenvalues are also decreasing as a consequence of the min-max theorem.

As explained before, the spectrum of $\mathbf{\Lambda}_\rho$ has 1 negative element and 3 positive elements when $\rho \to 0$ and 3 negative elements and 1 positive element when $\rho \to \infty$ [18]. Taking into account the monotonicity of the eigenvalues, it can be seen that two and only two eigenvalues change their sign. These two eigenvalues take a

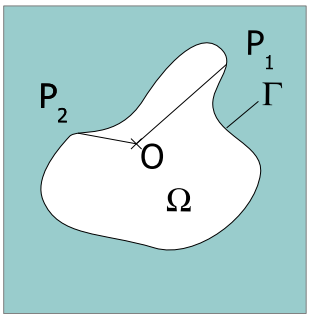

Fig. 4 Star-shaped boundary

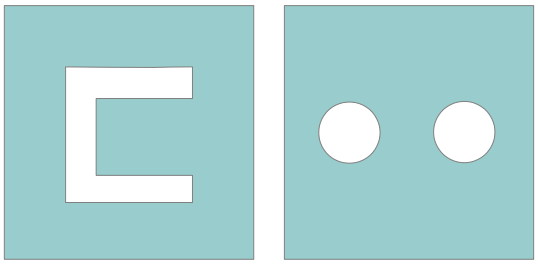

Fig. 5 Examples of non-star-shaped domains

zero value, leading to a non-invertible matrix Λ_ρ. Finally there are exactly two degenerate scales for such a star-shaped boundary.

We give here two examples of non-star-shaped domains (Fig. 5) that do not satisfy the condition of inclusion of homothetic domains in the original one.

The condition that the domain transformed by a homothety of ratio $0 < \rho < 1$ (though combined with a rotation) should be included in the original domain can be met also by some non-star-shaped domains as in the following example with logarithmic spirals (Fig. 6). In this case, the homothety of ratio inferior to 1 transforms an initial domain into a smaller one. Then, a rotation of this smaller domain produces a domain included within the initial one.

After a rotation of θ of the vectors of the basis, $\mathbf{\Lambda}$ is transformed into $\mathbf{\Lambda}_\theta$: $\mathbf{\Lambda}_\theta = \mathbf{R}^{-1}\mathbf{\Lambda}\mathbf{R}$ with:

$$\mathbf{R} = \begin{pmatrix} 1 & 0 & 0 & 0 \\ 0 & \cos(\theta) & \sin(\theta) & 0 \\ 0 & -\sin(\theta) & \cos(\theta) & 0 \\ 0 & 0 & 0 & 1 \end{pmatrix}, \tag{43}$$

and the eigenvalues of $\mathbf{\Lambda}$ and $\mathbf{\Lambda}_\theta$ are the same. Following the same path as for star-shaped boundaries, it can be shown that there are only two degenerate scales.

Costabel and Dauge [18] noticed that for connected curves, they could not find more than two degenerate scales. This is now proved for the special case of star-shaped curves.

4.4 A counter example for multi-connected boundary and its consequences

The numerical solution for the degenerate scales of two unit squares obtained by [18] has shown that if the distance between their centers is ≥ 20.97, there are four degenerate scales.

The fact that the matrix Λ_ρ has 1 negative eigenvalue and 3 positive eigenvalues for small ρ and 3 negative eigenvalues and 1 positive eigenvalue for large ρ has been proved under very general conditions in [18]. Then we conclude that, in that case, the decreasing property of the eigenvalues of $\mathbf{\Lambda}$ as a function of ρ does not hold.

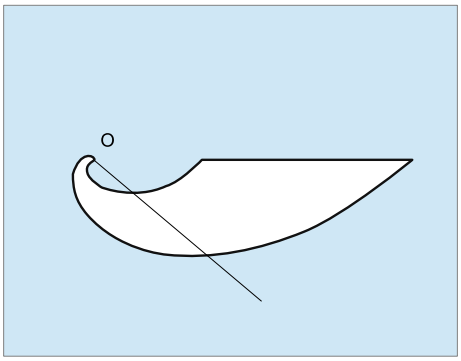

Fig. 6 Domain bounded by logarithmic spirals and a segment

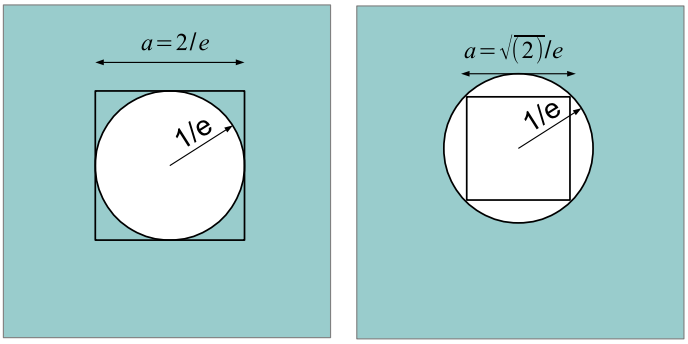

Fig. 7 Squares included or including the degenerate scale circle

4.5 Sufficient conditions for not being at a degenerate scale

A consequence is that for a star-shaped boundary, it is not possible to have 4 positive eigenvalues or 4 negative eigenvalues of $\mathbf{\Lambda}$. If we assume that there exists a scale ρ so that there are 4 negative or null eigenvalues, these eigenvalues decrease for increasing ρ and it is not possible to reach the limit case for large ρ with one strictly positive eigenvalue and three negative eigenvalues. Similarly, it can be shown that for a star-shaped boundary, it is not possible to have 4 positive or null eigenvalues.

We consider now a star-shaped boundary Γ' that is included in another one Γ which has 3 positive eigenvalues and one negative values. From the previous results, the eigenvalues Λ_Γ of the outer boundary are smaller than those of the matrix $\Lambda_{\Gamma'}$ of the inner one.

If the boundary Γ' was at a degenerate scale, $\Lambda_{\Gamma'}$ would have one zero eigenvalue and three positive ones, that is 4 positive or zero eigenvalues. But this is impossible, as has been shown above. Therefore, the inner boundary Γ' cannot be at a degenerate scale. Similarly if a boundary with 3 negative eigenvalues and 1 positive eigenvalues is included in a star-shaped boundary, this last boundary cannot be at a degenerate scale.

We can conclude that a star-shaped boundary included in a circle of radius $\leq 1/e$, or a star-shaped boundary containing a circle of radius $\geq 1/e$ is not at a degenerate scale.

We can deduce bounds for the degenerate scales of a square (see Fig. 7). The degenerate side length a of a square is such that:

$$0.5203 \approx \frac{\sqrt{2}}{e} \leq a \leq \frac{2}{e} \approx 0.7357. \tag{44}$$

This can be compared with the numerical value 0.60197 found in [18].

5 The discriminant matrix for symmetric domains and its consequence for a link with plane elasticity

5.1 Use of symmetry

The effect of the symmetry on the form of the discriminant matrix has been found for the case of a rectangle and for a rotation group of order ≥ 3 [18]. We elaborate here on these lines: we show that the discriminant matrix related to domains having defined symmetries degenerates to simpler forms for an appropriate coordinate system.

5.1.1 Eigenvectors of the discriminant matrix related to given symmetries

Case of an axis symmetry We assume that Ox_1 is a symmetry axis. Then there is at least one eigenvector of $\mathbf{\Lambda}$ with $A_2 \neq 0$ with the associated solution $u(x)$. Then we consider $w(x) = u(x) - u(\bar{x})$ with $\overline{(x_1, x_2)} = (x_1, -x_2)$. Due to the symmetry, w is also a solution of the augmented system (16) and we see that w is an odd function of x_2.

Then considering the asymptotic behaviour of w, we see that $w(x)$ is a solution with $A_i = 0$, $B_i = 0$, $i \neq 2$, and $A_2 \neq 0$, due to the fact that the corresponding terms are even function of x_2. Then the vector $(0, 0, 1, 0)$ is an eigenvector of $\mathbf{\Lambda}$.

Case of a point symmetry We assume now that the boundary has a symmetry center O. The symmetric matrix $\mathbf{\Lambda}$ has a basis of eigenvectors. It is possible to find 2 of these eigenvectors such that their components on Π (A_1, A_2), (A_1^*, A_2^*) are free. We consider now the function $u(x)$ corresponding to one of these eigenvectors, solution of (13), and the function $w(x) = (u(x) - u(-x))/2$. This is still a solution of the biharmonic problem and its asymptotic behaviour is $w(x) = -(A_1 x_1 + A_2 x_2)(\ln(r) + 2) - B_1 x_1 - B_2 x_2$. and similarly for the other eigenvector. Finally we conclude that these two eigenvectors are in the plane Π.

Case of a rotational symmetry of order $n \geq 3$ Costabel and Dauge [18] have stated that in that case (with Dirichlet boundary condition) there is always a double degenerate scale. We give here a detailed proof.

We consider a curve with a rotational symmetry of order $n \geq 3$. We consider one eigenvector having non-null components on Π: A_1, A_2. We consider the function $u(x)$ associated to this eigenvector with asymptotic behaviour defined by (13). We denote by Θ^j the rotation of angle $2j\pi/n$. We consider the function:

$$v'(x) = 2/n \sum_{j=0}^{n-1} \cos(j\pi/n) u(\Theta^j(x)). \tag{45}$$

Then an easy calculus shows that $v'(x)$ is associated to the eigenvector ($A'_0 = 0$, $A'_1 = A_1$, $A'_2 = A_2$, $A'_3 = 0$). The function $v'(\Theta^1(x))$ is associated to the eigenvector $(0, \Theta^1(\mathbf{A}), 0)$ with the same eigenvalue as $v'(x)$: there is a double eigenvalue and its eigen-space is Π.

5.1.2 Form of the matrix $\mathbf{\Lambda}$ for different symmetries

We consider the matrix $\mathbf{\Lambda}$ in the (O, Ox_1, Ox_2) coordinates. When Ox_1 is a symmetry axis we have the following form, using the symmetry:

$$\mathbf{\Lambda} = \begin{pmatrix} \Lambda_{00} & \Lambda_{01} & 0 & \Lambda_{03} \\ \Lambda_{01} & \Lambda_{11} & 0 & \Lambda_{13} \\ 0 & 0 & \Lambda_{22} & 0 \\ \Lambda_{03} & \Lambda_{13} & 0 & \Lambda_{33} \end{pmatrix}. \tag{46}$$

When Ox_1 and Ox_2 are symmetry axes we have the following form:

$$\mathbf{\Lambda} = \begin{pmatrix} \Lambda_{00} & 0 & 0 & \Lambda_{03} \\ 0 & \Lambda_{11} & 0 & 0 \\ 0 & 0 & \Lambda_{22} & 0 \\ \Lambda_{03} & 0 & 0 & \Lambda_{33} \end{pmatrix}. \tag{47}$$

If O is a point symmetry, the matrix $\mathbf{\Lambda}$ has the form:

$$\mathbf{\Lambda} = \begin{pmatrix} \Lambda_{00} & 0 & 0 & \Lambda_{03} \\ 0 & \Lambda_{11} & \Lambda_{12} & 0 \\ 0 & \Lambda_{12} & \Lambda_{22} & 0 \\ \Lambda_{03} & 0 & 0 & \Lambda_{33} \end{pmatrix}. \tag{48}$$

It is noticeable that the second and third rows and columns correspond to components of A_i and B_j along the axes. As a consequence, a rotation of axes transforms the central submatrix of $\mathbf{\Lambda}$ in accordance with the usual rotational transformation. The symmetric submatrix $\begin{pmatrix} \Lambda_{11} & \Lambda_{12} \\ \Lambda_{12} & \Lambda_{22} \end{pmatrix}$ has a system of orthogonal eigenvectors. If we take the corresponding directions as the new axes, the matrix (48) is reduced to (47). For a rotational symmetry of order $n \geq 3$, the form of the discriminant matrix is the same as for two axes of symmetry and in addition, $\Lambda_{11} = \Lambda_{22}$.

5.1.3 The degenerate scales for symmetric domains

In the case of a domain having only one symmetry axis x_1, matrix $\mathbf{\Lambda}$ has one obvious eigenvector $[V] = [0, 0, 1, 0]^T$ related to the third column. After the product by Ψ^{-1}, it can be seen that $[V]$ is again an eigenvector of the product with the eigenvalue $\lambda = -\Lambda_{22}/2$, that produces the degenerate scale $\rho = e^{-\lambda} = e^{\Lambda_{22}/2}$.

In the case of two symmetry axes, or a point symmetry, or a n-axis symmetry the matrix $\mathbf{\Lambda}$ can have the form Eq. (47), and we can write:

$$\Psi^{-1}\mathbf{\Lambda} = \begin{pmatrix} \Lambda_{03} & 0 & 0 & \Lambda_{33} \\ 0 & -\frac{1}{2}\Lambda_{11} & 0 & 0 \\ 0 & 0 & -\frac{1}{2}\Lambda_{22} & 0 \\ \Lambda_{00} & 0 & 0 & \Lambda_{03} \end{pmatrix}. \tag{49}$$

For finding the eigenvalues, we write:

$$|\Psi^{-1}\mathbf{\Lambda} - \lambda\mathbf{I_d}| = \left(\lambda + \frac{1}{2}\Lambda_{11}\right)\left(\lambda + \frac{1}{2}\Lambda_{22}\right)((\Lambda_{03} - \lambda)^2 - \Lambda_{00}\Lambda_{33})). \tag{50}$$

This equation has two obvious solutions $\lambda = -\frac{1}{2}\Lambda_{11}, -\frac{1}{2}\Lambda_{22}$, that are also obtained from the second and third column in (50). They produce again two degenerate scales $\rho_1 = e^{\Lambda_{11}/2}$, $\rho_2 = e^{\Lambda_{22}/2}$.

In addition, from Eq. (50), we see that there are only two degenerate scales, counting their multiplicities if $\Lambda_{00}\Lambda_{33} < 0$ (the related values of λ are complex) and four if $\Lambda_{00}\Lambda_{33} \geq 0$. In this case, the eigenvalues are given by: $\lambda = \Lambda_{03} \pm \sqrt{\Lambda_{00}\Lambda_{33}}$.

5.1.4 Condition for having monotonic relation between scale and the discriminant matrix

In the case of a domain having two symmetry axes, a point symmetry (using convenient axes, as explained before) or a n-axis symmetry we can evaluate $\mathbf{\Lambda}_\rho$ using (30):

$$\mathbf{\Lambda}_\rho = \begin{pmatrix} \rho^2\Lambda_{00} & 0 & 0 & \Lambda_{03} + \ln(\rho) \\ 0 & \Lambda_{11} - 2\ln(\rho) & 0 & 0 \\ 0 & 0 & \Lambda_{22} - 2\ln(\rho) & 0 \\ \Lambda_{03} + \ln(\rho) & 0 & 0 & \Lambda_{33}/\rho^2 \end{pmatrix}. \tag{51}$$

We aim at finding a condition for having $\mathbf{\Lambda}_\rho \downarrow$ when $\rho \uparrow$.

It is necessary and sufficient to check that:

$$\begin{aligned} P &= (A_0, 0, 0, A_3)\mathbf{\Lambda}_\rho(A_0, 0, 0, A_3)^T \\ &= A_0^2\rho^2\Lambda_{00} + 2A_0A_3(\Lambda_{03} + \ln(\rho)) + A_3^2\Lambda_{33}/\rho^2 \end{aligned} \tag{52}$$

decreases when $\rho \uparrow$ for all values of (A_0, A_3). We consider the derivative of P with respect to ρ and we denote $X = \rho A_0$, $Y = A_3/\rho$. We find the condition $X^2\Lambda_{00} + XY - Y^2\Lambda_{33} \leq 0$. For complying with this relation, it is necessary and sufficient that $\Lambda_{00} < 0$, $\Lambda_{33} > 0$ and $-\Lambda_{00}\Lambda_{33} \geq 1/4$. It can been noticed that for a circle these conditions are verified because in this case we have the equality $-\Lambda_{00}\Lambda_{33} = 1/4$.

5.1.5 Application to symmetric simply connected curves

The result of 5.1.3 can be used to show that a simply connected symmetric curve (2 symmetry axes, a point symmetry or a n-axis symmetry) has only two degenerate scales even if the domain is not star-shaped. We consider one circle included in the curve and one circle in which the curve is included. Then the coefficients Λ_{00} and Λ_{33} are decreasing when comparing the inner circle, the curve and the outer circle. From the values of $\Lambda_{00} = -R^2/2$ and $\Lambda_{33} = 1/(2R^2)$ for a circle of radius R, we deduce that we have $\Lambda_{00} < 0$ and $\Lambda_{33} > 0$ for the curve. As a consequence, there are only two degenerate scales, taking into account their multiplicity.

Therefore, the previous property of having two degenerate scales for star-shaped curves is extended to "symmetric" simple curves.

5.2 Use of a complex method for Lamé equation and biharmonic equation for the exterior domain of a simple curve

In this section we will compare the problem of plane elasticity and the biharmonic problem. The main link between the two problems is that the Airy stress function of plane elasticity satisfies a biharmonic equation; but there is no obvious analogy between the physical quantities related to the two problems.

5.2.1 Similarity between the complex formulation of the Dirichlet problems of plates and of plane elasticity

We consider the exterior problem of a simple curve. Without loss of generality, we assume that the origin of axes is located within the interior domain. A solution u of the biharmonic equation or the displacement (v_1, v_2) in elasticity plane can be expressed using complex functions:

$$v_1 - i\,v_2 = \kappa\bar{\Phi} - \bar{z}\Phi' - \Psi \text{ (Lamé equation)}, \tag{53}$$

$$u = \Re(\bar{z}\phi(z) + \psi(z)) \text{ (biharmonic equation)}. \tag{54}$$

The expression of the homogeneous Dirichlet boundary condition is quite similar for Lamé equation and biharmonic equation when using Goursat's functions [42,44]:

$$\kappa\bar{\Phi} - \bar{z}\Phi' - \Psi = 0,\ z \in \Gamma \text{ (Lamé equation)}, \tag{55}$$

$$\bar{\phi} + \bar{z}\phi' + \psi' = 0,\ z \in \Gamma \text{ (biharmonic equation)}. \tag{56}$$

The Eq. (56) ensures that $\frac{\partial u}{\partial n} = 0$ on Γ and that $u = \Re(\bar{z}\phi(z) + \psi(z))$ is constant on Γ. Then, for homogeneous Dirichlet condition, it is necessary to add to (56) the following condition:

$$u = \Re(\bar{z}\phi(z) + \psi(z)) = 0, \quad z \in \Gamma. \tag{57}$$

If a boundary is at the degenerate scale for Lamé equation with the complex fundamental solution, there are a complex constant A and two holomorphic functions Φ, Ψ, such that: $\Phi = A\ln(z) + \Phi_0(z)$; $\Psi = -\kappa\bar{A}\ln(z) + \Psi_0$ and $\Psi_0 \to 0$, $\Phi_0 \to 0$ when $|z| \to \infty$ and satisfying (55) [7,15]. If $A = re^{i\theta}$, the resultant force has an angle θ with Ox_1. It should be noticed that κ is equal to $3 - 4\nu$ with ν the Poisson's ratio for the plane elasticity problem; the degenerate scales for the plate problem with Dirichlet boundary condition do not depend on the Poisson's ratio of the plate material.

If Eqs. (56, 57) are both satisfied on the boundary, then u is a solution of the homogeneous Dirichlet biharmonic problem.

Eqs. (55, 56) are the same if $\kappa = -1$, $\phi = \Phi$ and $\psi' = \Psi$ or $\kappa = 1$ and $\phi = i\,\Phi$ and $\psi' = i\,\Psi$.

5.2.2 Case of a symmetry axis

We consider now an exterior biharmonic problem. It has been shown in Sect. 5.1.3 that a suitable change of scale can transform an initial $\mathbf{\Lambda}$ matrix into a singular matrix $\mathbf{\Lambda}_i$ for each degenerate scale ρ_i. We assume that (O, x_2) is a symmetry axis, so that (0, 1, 0, 0) is the eigenvector of $\mathbf{\Lambda}_1$ related to a null eigenvalue of $\mathbf{\Lambda}_1$ Sect. 5.1.3. As a consequence, the scaled boundary is at a degenerate scale for the Dirichlet biharmonic problem and the related

eigenfunction has the following behaviour at infinity: $u = x_1(2\ln(r)+1)+c_1\cos(2\theta)+c_2\sin(2\theta)+O(1/r)$. Then Goursat's functions can be written as:

$$\phi = \ln(z) + (c_1 + ic_2)\frac{1}{z} + \phi_0(z), \quad \psi = z\ln(z) + z + d + \psi_0(z), \tag{58}$$

with

$$u = \Re\left(\bar{z}\phi(z) + \psi(z)\right). \tag{59}$$

The Goursat functions are not uniquely determined, in particular ϕ is determined up to $\alpha z + \beta$ with $\alpha \in \mathbb{R}$ and $\beta \in \mathbb{C}$ [37, p. 179]. Functions ϕ_0 and ψ_0 are holomorphic functions such that $\phi_0 = O(1/r^2)$ and $\psi_0 = O(1/r)$.

It should be noticed that we assume here that the domain is bounded by a simple curve with the origin inside this curve. For an exterior domain bounded by several simple curves Γ_i, it is necessary to consider extra terms like $\ln(z - z_i)$, $z\ln(z - z_i)$ with z_i inside Γ_i (See Sect. 5.4).

Then, the following equation is satisfied on Γ:

$$\bar{\phi} + \bar{z}\phi' + \psi' = 0, \tag{60}$$

with $\psi' = \ln(z) + 2 + \psi_0'$.

We define:

$$\tilde{\Phi}(z) = i(\phi(z/e) + 1), \quad \tilde{\Psi}(z) = i(\psi'(z/e) - 1). \tag{61}$$

.

We write the complex expression of Lamé Eq. (55) for $\tilde{\Phi}$, $\tilde{\Psi}$ and $\kappa = 1$:

$$\begin{aligned}\overline{\tilde{\Phi}(z)} - \bar{z}\tilde{\Phi}'(z) - \tilde{\Psi}(z) &= -i\,\overline{\phi(z/e) + 1} - \bar{z}\frac{i}{e}\phi'(z/e) - i(\psi'(z/e) - 1) \\ &= -i\left(\overline{\phi(z/e)} + (\frac{\bar{z}}{e})\phi'(z/e) + (\psi'(z/e))\right).\end{aligned} \tag{62}$$

We denote by Γ_e the boundary which is homothetic to Γ with ratio e. From (62), we conclude that Eq. (55) is satisfied by $(\tilde{\Phi}, \tilde{\Psi})$ on Γ_e if Eq. (56) is satisfied on Γ by (ϕ, ψ).

Let us check that the asymptotic behaviours of $(\tilde{\Phi}, \tilde{\Psi})$ satisfy the requirements for finding the degenerate scales in plane elasticity:

$$\tilde{\Phi}(z) = i(\phi(z/e) + 1) = i(\ln(z/e) + \phi_0(z/e) + 1) = i\ln(z) + i\phi_0(z/e), \tag{63}$$

$$\tilde{\Psi}(z) = i(\psi'(z/e) - 1) = i(\ln(z/e) + 2 + \psi_0'(z/e) - 1) = i\ln(z) + i\psi_0'(z/e). \tag{64}$$

Finally, we can conclude that the boundary Γ_e is at a degenerate scale for elasticity with a resultant force in Ox_2 direction. The degenerate scale for the biharmonic equation is therefore equal to $1/e$ times the degenerate scale for plane elasticity (for the standard complex fundamental solution that is different from the Kelvin fundamental solution).

5.2.3 Other cases

If the curve is a simple one and has a point symmetry or two symmetry axes or a rotational symmetry, then there are only two degenerate scales and the problem of the degenerate scale for the biharmonic equation is reduced to the case of elasticity.

Remarks

- It is questionable whether it is possible to extend this method to the other two possible degenerate scales of the biharmonic problem or not. This does not seem possible because at least one of the corresponding eigenvectors would have a term $r^2\ln(r)$ which results for the elasticity problem in a term $r\,ln(r)$ which grows too fast for the elasticity representation formula.
- The condition of having only one symmetry axis gives the link between one degenerate scale of the biharmonic problem and one degenerate scale of the plane elastic problem. This condition is not sufficient to have the link between two degenerate scales for plane elasticity and for plates. This is proved by the example of an arc of circle in Sect. 7.

5.3 Extension of previous results on elasticity to the biharmonic equation

This link between elasticity and biharmonic problem allows us to find exact values of the degenerate scales of biharmonic Dirichlet problem when the boundary is a simple curve with symmetries if the degenerate scales for plane elasticity are known. A direct application is the case of the circle of radius 1. We recover the degenerate scale e^{-1} found in Ref. [18]. For a segment of length 4, the degenerate scales for biharmonic equation are found as $e^{-3/2}$, $e^{-1/2}$ [18]. The degenerate scale for plane elasticity using the fundamental solution issued from complex methods are $e^{-1/2}$, $e^{1/2}$ [54]. The ratio e^{-1} is also verified for the segment.

5.3.1 Comparison with previous numerical results: case of an ellipse

As a third example, we consider the ellipse with half axes a, b. If $a + b = 2$ then the degenerate scales for plane elasticity are $e^{\pm m/2\kappa}$ with $m = (a - b)/(a + b)$ [7]. Then the degenerate scale for the Dirichlet biharmonic problem is $e^{-1\pm m/2}$. We can evaluate the values for the case $b = a/2$ considered in [5] for a numerical evaluation. We choose $a = 4/3$, $b = a/2 = 2/3$ to comply with $a + b = 2$ and we get $m = 1/3$. The degenerate scales for elasticity are $e^{-1/6\kappa}$, $e^{1/6\kappa}$; for Dirichlet biharmonic equation the degenerate scales are $e^{-7/6}$, $e^{-5/6}$. It leads to the values of the minor semi-axis $2/3e^{-7/6} \approx 0.2076$, $2/3e^{-5/6} \approx 0.2897$. The agreement is excellent with the values found numerically [5]: (0.2077, 0.2899).

5.3.2 Use of a rational conformal mapping

When the outside of a boundary is the image of the outside of the unit circle by a rational fraction, it is possible to find the closed form of the degenerate scales for plane elasticity [15]. Of course, this implies that the boundary is a simply connected curve. The proof still holds for $\kappa = (3 - 4\nu) = 1$. Then, if the boundary has also the required symmetries, the value of the degenerate scales for Dirichlet biharmonic equation can also be found. For numerous cases, the calculus has been carried out completely [8,15].

5.3.3 Inequalities and bounds

If we assume that the degenerate scales for elasticity are continuous when $\nu \to \frac{1}{2}$, then these degenerate scales for biharmonic equations inherit properties from the degenerate scales obtained in plane elasticity.

Lower bound From [16], we deduce: $\rho_0 e^{-3/2} \leq \rho_i$, ρ_0 is the degenerate scale factor for Laplace equation and $\rho_i, i = 1, 2$ are the degenerate scale factors for the biharmonic equation.

Upper bounds From [14], we deduce: $\min\{\rho_i\} \leq \rho_0 e^{-1}$; $\max\{\rho_i\} \leq \rho_0 e^{-1/2}$; $\rho_1 \rho_2 \leq \rho_0^2 e^{-2}$.

These bounds are all expressed by using the degenerate scale for Laplace equation ρ_0, itself coming from the logarithmic capacity, that is largely documented.

Case of one domain included in another one The fact that the degenerate scales are larger for the domain included within another one could also be directly deduced from the same property for plane elasticity [14].

5.4 Case of an exterior domain with two bounded boundaries

For a multi-connected domain, the Goursat functions ϕ and ψ for a biharmonic function must be written with some extra terms compared with the case of a simply connected domain (Eq. 58):

$$\phi(z) = \sum_{k=1}^{n} \alpha_k z \ln(z - z_k) + \sum_{k=1}^{n} \beta_k \ln(z - z_k) + \phi^*(z), \tag{65}$$

$$\psi = \sum (\gamma_i z \ln(z - z_i) + \delta_i \ln(z - z_i)) + \psi^*, \tag{66}$$

where $\phi^*(z)$, $\phi^*(z)$ are uni-valued holomorphic functions and z_k is an interior point of the interior domain bounded by Γ_k [37, p. 182]. For $\Re(\bar{z}\phi + \psi)$ being univalent, we need that $\alpha_i, \delta_i \in \mathbb{R}$ and $\beta_i = \overline{\gamma_i}$.

Then the coefficient of the term in $r^2 \ln(r)$ when $r \to \infty$ is equal to $\sum_{k=1}^{n} \alpha_k$.

For having the correspondence between solutions of the plate problem and of the plane elasticity problem, it is needed more: all α_i must be null to find the ϕ related to the solution of an elastic problem [43, p. 124].

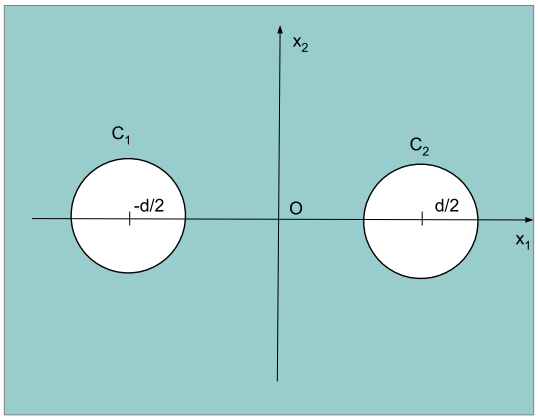

Fig. 8 Case of two circles

When we are looking for eigenvalues related to (0, 1, 0, 0) and (0, 0, 1, 0), we have $\sum_{k=1}^{n} \alpha_k = 0$. If there is only one interior boundary Γ_1, we deduce $\alpha_1 = 0$. And so the expression is compatible with the complex solution of an elasticity problem. This case has been addressed in the preceding section.

There is no obvious extension of this result in the general case of multi-connected domains. An extension can be performed in the case of domains having specific symmetries, as described thereafter.

We consider the case with two symmetry axes, for instance two equal circles (Fig. 8) and look at the solution associated with (0, 0, 1, 0). We know from Sect. 5.1 that the related solution is odd with respect to x_2. Due to the double symmetry, this solution is even with respect to x_1 (it is possible to replace $u(x_1, x_2)$ by $(u(x_1, x_2) + u(-x_1, x_2))/2$, which has the same asymptotic behaviour as u).

Then $\alpha_1 = \alpha_2$ and $\alpha_1 + \alpha_2 = 0$ and so $\alpha_1 = \alpha_2 = 0$. Therefore, the holomorphic functions in the Goursat formula for u are compatible with an elasticity solution. It means that the related degenerate scale can be found from one of those corresponding to the elasticity problem.

It should be noticed that this argument fails for the solution associated to (0, 1, 0, 0). This solution is odd with respect to x_1 (and even with respect to x_2). This leads to $\alpha_1 = -\alpha_2$. The two axes play a different role (see Fig. 8): the symmetry along the Ox_2 axis changes C_1 into C_2 and the symmetry along the Ox_1 axis changes C_i into itself.

Some cases (2 equal segments, 2 symmetric arcs of one circle) are analytically solved [15] for the elasticity problem, and so one of the degenerate scale for the biharmonic problem can be deduced. When the distance d between the two boundaries increases, it has been proved that the "elastic" degenerate scales behave as $d^{-1/2}$ [53]. This behaviour has been found numerically for some of the "biharmonic" degenerate scales of two distant squares [18]. For the case of 2 circles, the asymptotic values of "elastic" degenerate scale are given in [53], that produces the asymptotic behaviour of one of the degenerate scales for plates.

6 Some consequences for the biharmonic outer radius

6.1 Definition of the biharmonic outer radius

Pólya and Szegö introduced a biharmonic function $\bar{\Gamma}$ (see [46, p. 141] and also [45]):

$$\bar{\Gamma}(x) = \log(1/|x|) + ar^2 + b_1 x_1 + b_2 x_2 + \bar{h}, \ |x| \to \infty, \tag{67}$$

with $\bar{\Gamma} = 0$, $\frac{\partial \bar{\Gamma}}{\partial n} = 0$, on the boundary and $\bar{h}$ being a bounded biharmonic function. Using Sect. 3.2, we can deduce that $a = \Lambda_{33}$. For the circle, the same authors give $\bar{\Gamma} = \ln\left(\frac{R}{|x|}\right) - \frac{(R^2 - |x|^2)}{2R^2}$. This corresponds to the value of the last column of the discriminant matrix $\mathbf{\Lambda}$ for a circle, as seen in (35).

Pólya and Szegö stated that $a > 0$ (or equivalently $\Lambda_{33} > 0$) and defined the biharmonic outer radius $\bar{s}$ by $\bar{s} = 1/\sqrt{2a}$ (see also [45]). From Eq. (67), it can be readily seen that the biharmonic outer radius does not depend on the origin of the axes nor on a rotation of the axes. These authors proved that, for nearly circular curves, the biharmonic outer radius is greater or equal to the conformal radius (the degenerate scale factor for

the Laplace equation is reached when the conformal radius is equal to 1). For the circle, the biharmonic outer radius is found equal to R and then equal to the conformal radius. It should be noticed that this biharmonic radius is different from the N-harmonic radius defined in [55].

6.2 Some results on the biharmonic outer radius

The result of Sect. 4 concerning $\mathbf{\Lambda}$ has interesting consequences concerning the biharmonic outer radius.

First, a boundary included in one circle has its coefficient Λ_{33} greater or equal to the coefficient Λ_{33} of the circle, which has been found equal to $1/2R^2 > 0$. An alternative proof can also be deduced from the minimizing problem of Sect. 3.3 by using the fact that $J(\phi_3, \phi_2) \geq 0$ if $p_0 = p_1 = p_2 = 0$. This proves the existence of the biharmonic outer radius. This is also true for multi-connected boundaries.

Second, this also proves that if one curve is included within another, then the outer biharmonic radius of the first is less than or equal to the outer biharmonic radius of the second.

These two results concern only the biharmonic problem and other problems investigated in [46] are not considered here.

7 Computation of degenerate scales by boundary elements and numerical examples

We intend now to verify some features of the degenerate scale for plates by using a boundary element formulation.

7.1 Boundary element formulation

We start from the integral Eq. (11) and we denote $E_0(x, y) = 8\pi E(x, y)$.

The augmented system of boundary integral equations writes:

$$\int \left(E_0(x, y)\phi_3 + \frac{\partial E_0}{\partial n_y}(x, y)\phi_2 \right) \mathrm{d}S_y = \sum_0^3 B_i q_i(x), \tag{68}$$

$$\int \left(\frac{\partial E_0}{\partial n_x}(x, y)\phi_3 + \frac{\partial^2 E_0}{\partial n_y \partial n_x}(x, y)\phi_2 \right) \mathrm{d}S_y = \sum_0^3 B_i \frac{\partial q_i}{\partial n_x}(x), \tag{69}$$

$$\int \left(\phi_3 q_i + \phi_2 \frac{\partial q_i}{\partial n_x} \right) \mathrm{d}S_y = A_i, i = 0..3; \tag{70}$$

with

$$q_0 = 1, \quad q_1 = x_1, \quad q_2 = x_2, \quad q_3 = x_1^2 + x_2^2. \tag{71}$$

Using boundary elements, the system can be written:

$$\begin{bmatrix} A' & B' & G \\ C & D & H \\ E & F & 0 \end{bmatrix} \begin{bmatrix} \phi_3 \\ \phi_2 \\ \mathbf{B} \end{bmatrix} = [V], \tag{72}$$

with

$$[V] = \begin{bmatrix} 0 \\ 0 \\ \mathbf{A} \end{bmatrix}, \quad [\mathbf{B}] = \begin{bmatrix} B_0 \\ B_1 \\ B_2 \\ B_3 \end{bmatrix}, \quad [\mathbf{A}] = \begin{bmatrix} A_0 \\ A_1 \\ A_2 \\ A_3 \end{bmatrix}. \tag{73}$$

where $[\phi_2]$, $[\phi_3]$ are values of functions ϕ_2, ϕ_3 at nodal points $\mathbf{x}_j$.

The interaction matrices $\left[A'\right]$, $\left[B'\right]$, ... can be obtained after having chosen the interpolation functions for ϕ_2, ϕ_3. In the course of this study, two kinds of interpolation functions have been used. In a first step, we have

Table 1 Degenerate scales ρ_{plate} for plates of connected contours and comparison with the "elastic" degenerate scales ρ_{elas}

Shape	Nb. elts	ρ_{plate}	$e.\rho_{\text{plate}}$	ρ_{elas}	Rel. err.	Refs.
Circle $R = 1$	200	0.368	1.0004	1	4.0E−04	[44]
Square $a = 1$	200	0.602	1.6365	1.6372	3.9E−04	[44]
Eq. Triangle $a = 1$	300	0.818	2.2227	2.2222	3.3E−04	[44]
Star	400	0.147	0.3989	0.3993	9.5E−04	Num.
Arc of circle $\alpha = \pi/4$	200	1.167	3.1722	3.1687	1.1E−03	[44]
		3.053	8.3001	8.0044	3.6E−02	
Arc of circle $\alpha = \pi/2$	200	0.628	1.7071	1.7053	9.7E−04	[44]
		1.456	3.9570	3.5905	9.3E−02	

For the first four contours, the common value $\rho_{11} = \rho_{22}$ is reported. The relative error is computed between $e.\rho_{\text{plate}}$ and ρ_{elas}. The 4-pointed star is built on a square of side 1 and triangles whose outward vertices are on a circle of radius 3. For the arcs of circle, the two degenerate scales are reported and compared to the "elastic" ones

used constant interpolation functions on boundary segments. However, the nature of ϕ_3 corresponds to the normal derivative of the internal function leading to the boundary values of ϕ_2. This led Costabel and Dauge [25] to use different interpolations for these two functions, ϕ_2 being piecewise constant with centered nodes $\mathbf{x}_j$ and ϕ_3 being a sum of collocation functions, i.e. Dirac functions at each end point $\mathbf{z}_j$ of each constant element. The first integral equation is written at each end point $\mathbf{z}_i$ and the second integral equation is written at each node $\mathbf{x}_i$ located at the center of each element. The results presented in the next subsection have been obtained using this second method. The components of each submatrix $\left[A'\right], \left[B'\right], \ldots$ are described in appendix C. Matrix Λ is obtained by solving numerically the four linear systems related to the four values of A_i given by $A_i = \delta_{il}$ for $l = 1 \ldots 4$.

7.2 Numerical results and comparison with some analytical results

7.2.1 Results for connected domains

In a first step, we look at the degenerate scales of four connected domains with at least two axes of symmetry or n-axis symmetry: circular, squared, triangular, star. The three first ones are convex and the fourth is star-shaped with the meaning of Sect. 5.2. We present also the results obtained for arcs of circle, with angles $\pi/4$ and $\pi/2$, which have only one symmetry axis, axis x_1. The comparison is made with the values obtained from the "elastic" degenerate scales as found in Sect. 6.2 by the relation $\rho_{\text{plate}} = \rho_{\text{elastic}}/e$ with $\nu = 0.5$ (i.e. $\kappa = 1$) for the elastic calculus. It is worthwhile recalling that the "elastic" degenerate scales to compare with the "plate" degenerate scales are those obtained for a Green's tensor coming from the complex formulation. These degenerate scales differ from the ones obtained from the usual Kelvin elastic Green's tensor by a factor $e^{1/2\kappa}$ [41,44]. The "elastic" degenerate scales are obtained either analytically when available (references given in Table 1) or numerically in other cases. All results are presented in Table 1. It can be seen that, for doubly symmetric or 3-axis symmetry domains, all degenerate scales are recovered from the "elastic" degenerate scale. For the equilateral triangle, the 3-axis symmetry induces that the two degenerate scales are the same.

In the case of the arc of circle, only one degenerate scale is recovered: the one corresponding to the symmetry with respect to axis x_1. The relative difference between the values obtained for the other one reaches nearly 0.1, that is largely higher than the numerical accuracy. For all these results, it has been checked that the form of matrix $\mathbf{\Lambda}$ is consistent with the form obtained for each symmetry in Sect. 6.1.

In addition to these results, two other cases have been studied. First, it has been verified that the case of a parallelogram having only a central symmetry and no symmetry axis produces two different degenerate scales. It has been shown that the form of the matrix $\mathbf{\Lambda}$ in this case is the one obtained in Sect. 5.1.2 leading to degenerate scales ρ_{elas}/e.

Table 1 presents the results for an equilateral triangle. It has the 3-axis symmetry but also 3 axes of symmetry, that is not conclusive for the case of a pure 3-axis symmetry. To complete these results, we have studied a domain having a 3-axis symmetry but no axis of symmetry. We have recovered again that the form of the matrix $\mathbf{\Lambda}$ is the one predicted in Sect. 5.1.2 with two identical degenerate scales and that the "plate" degenerate scales are consistent with elastic ones.

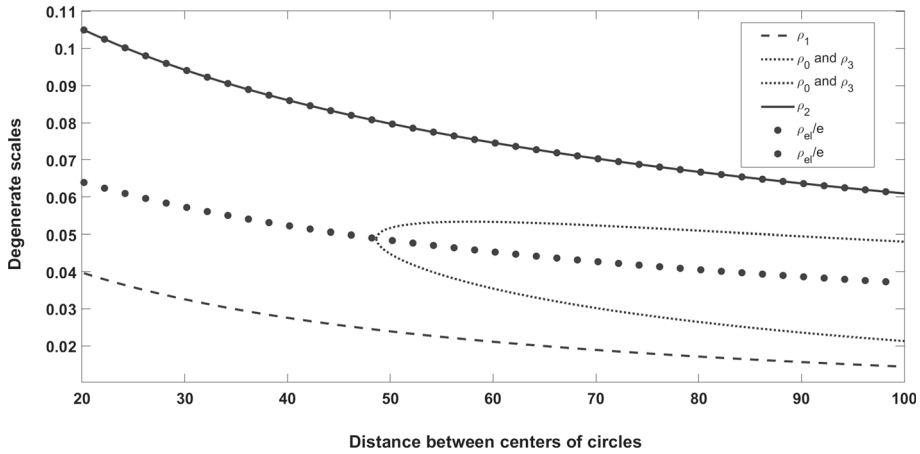

Fig. 9 Degenerate scales for two circles of radius 1 (symmetric with respect to x_2 and centered on x_1) as functions of an increasing distance between the centers of circles. ρ_1 and ρ_2 are the degenerate scales for plates related to Λ_{11} and Λ_{22}

7.2.2 Results for not simply connected domains

We have recovered the results on degenerate scales obtained by Costabel and Dauge [18] on a set of two squares whose distance d between centers is increasing. We recover notably that 4 degenerate scales are obtained when $d > 20.97$.

Case of two circles We present in Fig. 9 the results obtained for the case of two circles of radius 1 with increasing distance between their centers. It can be seen that similar results to the case of squares are obtained, but in this new case 4 degenerate scales are found when $d > 48.6$.

A comparison is made with the "elastic" degenerate scales. To do this, the plate degenerate scales are denoted by ρ_1 for the value related to Λ_{11} and similarly for ρ_2. The other two degenerate scales cannot be distinguished. They are denoted by ρ_0 and ρ_3. It can be seen that only one "elastic" degenerate scale is consistent with a degenerate scale for plate, the one corresponding to axis Λ_{22} (symmetry with respect to x_1). The other ones are completely different from the value obtained from the other "elastic" degenerate scale. This corresponds to what was suspected in Sect. 5.4.

It is worthwhile noticing that the numerical computations do not show the same asymptotic behaviour for ρ_1 and ρ_2. ρ_1 and one of ρ_0, ρ_3 behave as $1/d$, but ρ_2 and the other value of ρ_0, ρ_3 behave as $1/\sqrt{d}$. The latter is consistent with the asymptotic behaviour of the elastic degenerate scales, as found in Ref. [53].

Case of two segments A similar result is obtained in the case of two segments of length 1 located on x_1 and symmetrically with respect to x_2, with a distance $d = 6$ between the centers of segments. The value of $e.\rho_{22}$ is equal to $\frac{2}{\sqrt{d}} \cdot e^{1/2}$ that is the analytical solution for one of the degenerate scales. The value of $e.\rho_{11}$ is different from the second "elastic" degenerate scale, with a relative difference being around 40%.

Case of four arcs of circle A third series of results on a non-connected boundary is presented in Fig. 10 for doubly symmetric sets of four arcs of circles ($R = 1$) of increasing angle whose axes of symmetry are the coordinate axes. In this case, there is only one degenerate scale, due to the symmetry. It can be seen that the "elastic" degenerate scale is not consistent with the degenerate scale for plates except in the limit case of a full circle. It confirms that the correspondence between "elastic" degenerate scales and "plate" degenerate scales cannot be generally applied to the case of non-connected domains.

Case of 3 aligned circles Numerical results have been obtained also in the case of 3 aligned equidistant circles of unit radius. It has been found in this case that the behaviour of this domain is entirely different from the case of two circles only, leading always to only two degenerate scales.

This can be explained in the following way. We consider the matrix $\mathbf{\Lambda}$ for the 3 circles as the solution of the minimization problem (23); when we remove the 2 side circles, this is equivalent to add additional constraints $\phi_3 = \phi_2 = 0$ on the two side circles. Adding supplementary constraints to the minimization problem leads to a result that is greater or equal to the one related to the original solution. This is true for any choice of $(A_0, \mathbf{A}, A_3)$ and we deduce that the new matrix Λ' (corresponding to the central circle) is greater or equal to that of the 3 circles. For a circle whose center is at the origin of the coordinates, we have $\Lambda'_{00} < 0$, and so for the three circles we also have $\Lambda_{00} < 0$. This proves that there are only two degenerate scales, since

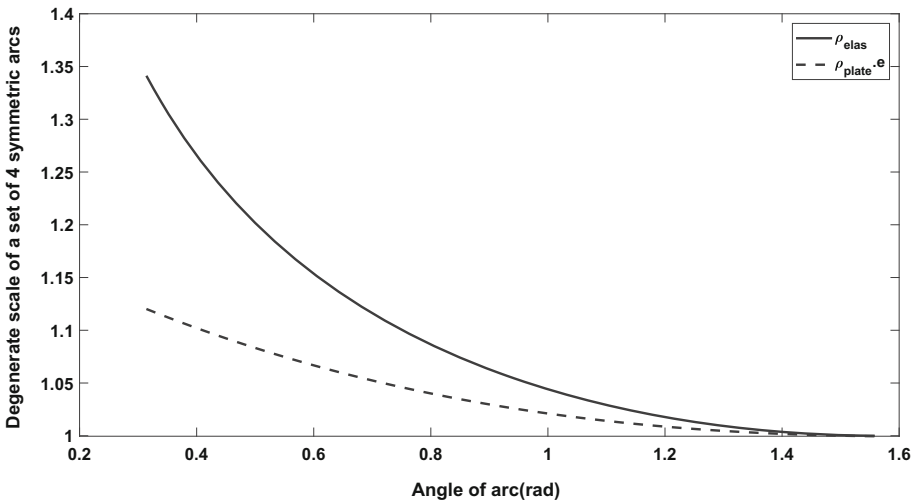

Fig. 10 Comparison of the degenerates scales for sets of four arcs of circles with the "elastic" ones. The degenerates scales are given as a function of one of the arcs (in rad). The value $\rho = 1$ is obtained for the full circle, i.e. four arcs of $\pi/2$ rad

there are two symmetry axes. It is worthwhile noticing that this argument cannot be applied to the case of two circles because the form of the discriminant matrix changes if the origin is set within one of the two circles. Therefore, it can be seen that the absence of third and fourth degenerate scales for three circles is due mainly to the existence of the central circle.

7.2.3 Monotonous behaviour of the discriminant matrix

As shown in Sect. 4, the discriminant matrix is a monotonous function for increasing domains. To check this property, we have computed the eigenvalues of the difference $d\mathbf{\Lambda}$ of the discriminant matrices of two domains, one contained within another. If the variation of $\mathbf{\Lambda}$ is monotonous, it means that the smallest eigenvalue $d\lambda_{\min}$ of $d\mathbf{\Lambda}$ is always of the same sign. We present therefore in Fig. 11 the variation of $d\lambda_{\min}$ for a set of circles that contain a square of unit side. It can be seen that $d\lambda_{\min}$ is always of the same sign, which confirms the monotonous behaviour of the discriminant matrix. As seen before, the behaviour of non-simply connected boundaries differs significantly from the one of simply connected ones. To check again the monotony property in the case of non-connected boundaries, we present in Fig. 11 the variation of $d\lambda_{\min}$ for a second example related to a set of increasing circles containing two circles of radius one whose centers are distant of $d = 4$. It can be seen that the monotonous behaviour of discriminant matrices is still verified in this case.

8 Conclusion

The behaviour of the degenerate scales of the biharmonic equation is much more complicated than for the Laplace or Lamé problem. For interior problems, we show that holes in a bounded domain have no influence on degenerate scales, that generalizes similar results obtained in the case of Laplace equation or plane elasticity. Following Costabel and Dauge [18], the degenerate scales are obtained by using a discriminant matrix $\mathbf{\Lambda}$ that is evaluated by using three different ways, including a new minimization problem and a boundary value problem for exterior domains related to a specific behaviour at infinity. The study of the properties of the discriminant matrix provides information on degenerate scales.

If a boundary is included in a larger simply connected boundary, the corresponding discriminant matrix $\mathbf{\Lambda}$ is larger than the $\mathbf{\Lambda}$ matrix of the largest domain. We have shown that for "star-shaped" boundaries, there are only two degenerate scales; for these domains it is possible to find sufficient conditions for not being at a degenerate scale.

The cases of boundaries having specific symmetries allow us to find additional properties. For a simply connected curve with two axes of symmetry or a point symmetry or n-axis symmetry, it is shown that there are only two degenerate scales. We have proved that these two degenerate scales are equal to the degenerate

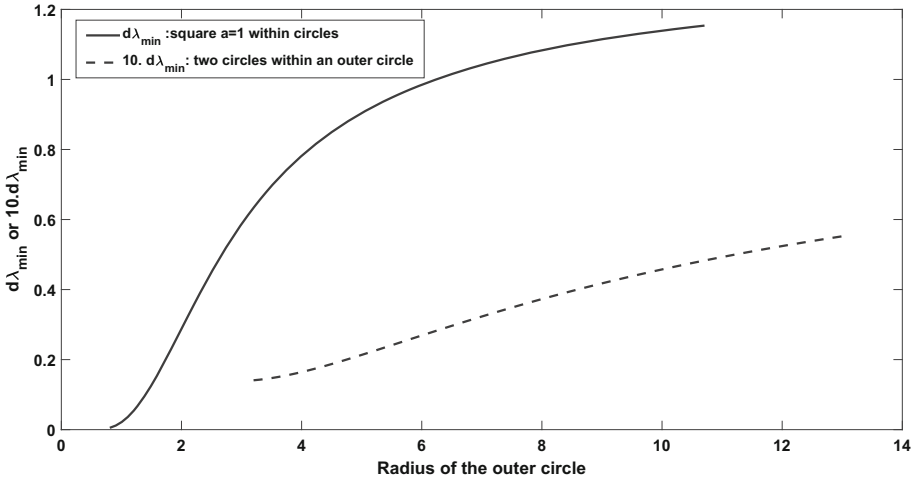

Fig. 11 Variation of the smallest incremental eigenvalue $d\lambda_{\min}$ as a function of the radius of increasing circles containing the square of side equal to 1 or a set of two circles of radius 1 with $d = 4$ between the centers

scales of plane elasticity of the same domain up to a multiplicative factor e. Numerical results confirm this set of results and show that these latter results cannot be generally extended to multi-connected domains.

The biharmonic outer radius defined by Pólya and Szegö turns out to be defined for simply connected and multi-connected domains. If one domain is included in another, its biharmonic outer radius is smaller than the one of the larger domain.

For practical applications involving BEM, the results allow us to find a condition on the size of the boundary preventing the occurrence of the degenerate scales in the case of a finite or an infinite domain bounded by a simple curve. This condition is proved if the domain inside the simple curve is star shaped or with two symmetry axes or a point symmetry or a n-axial symmetry. It can be conjectured that this is also true in the general case of a simple curve. The more elementary way to find a non-degenerate scale is to consider a scale such that the simple curve is included in a circle of radius $1/e$ or if a circle of radius $1/e$ is included in the domain bounded by the simple curve. In the case of a bounded domain, the holes have no influence on the degenerate scales; for an unbounded, non-simply connected domain, no general conclusion can be drawn. Our results have been checked by many comparisons between our theoretical results and our numerical results and with the results of previous authors, notably in Sect. 7.2.

For the present, the study has been concentrated on the case of Dirichlet boundary conditions corresponding practically to clamped plates with possible given displacement or rotations at the boundary. Obviously, many engineering situations involve mixed boundary conditions that are outside the scope of the paper, for example in the case of simply supported plates or free edge on a part of the boundary. Our previous studies in plane elasticity have shown that the case of Dirichlet boundary condition can be considered as a reference case for studying more intricate boundary conditions. For plates, we intend to produce a future study that will be devoted to the case of more general boundary conditions.

Appendix A: Integral equations for plates

We give here the four integral equations that can be used in the case of the interior problem. For more details see for example [29,30]. We complete Eq. (8) written for Dirichlet boundary condition by adding the terms needed for more general cases:

$$
\begin{aligned}
&(1)\int_\Gamma (E(x,y)\phi_3(y)+\frac{\partial E}{\partial n_y}(x,y)\phi_2(y)-M_y(E)(x,y)\phi_1(y)\\
&\quad -N_y(E)(x,y)\phi_0(y))\mathrm{d}S_y=\frac{1}{2}\phi_0(x);\\
&(2)\int_\Gamma \left(\frac{\partial E(x,y)}{\partial n_x}\phi_3(y)+\frac{\partial E(x,y)}{\partial n_x\partial n_y}(x,y)\phi_2(y)-\frac{\partial M_y(E)(x,y)}{\partial n_x}\phi_1(y)\right.\\
&\quad \left.-\frac{\partial N_y(E)(x,y)}{\partial n_x}\phi_0(y)\right)\mathrm{d}S_y=\frac{1}{2}\phi_1(x),
\end{aligned}
\tag{74}
$$

with

$$
E(x,y)=\frac{1}{8\pi}r^2\ln(r)\quad\text{with}\quad r=\sqrt{(x_1-y_1)^2+(x_2-y_2)^2}. \tag{75}
$$

Here ϕ_3 is the shear force, ϕ_2 the bending moment, ϕ_1 the rotation and ϕ_0 the normal displacement. Eqs. 3 and 4 are obtained by applying M_x and N_x to (1).

$$
\begin{aligned}
&(3)\int_\Gamma (M_x(E(x,y))\phi_3(y)+M_x\left(\frac{\partial E}{\partial n_y}(x,y)\right)\phi_2(y)\\
&\quad -M_x(M_y(E)(x,y))\phi_1(y)-M_x(N_y(E)(x,y))\phi_0(y))\mathrm{d}S_y=\frac{1}{2}\phi_3(x);\\
&(4)\int_\Gamma (N_x(E(x,y))\phi_3(y)+N_x\left(\frac{\partial E}{\partial n_y}(x,y)\right)\phi_2(y)\\
&\quad -N_x(M_y(E)(x,y))\phi_1(y)-N_x(N_y(E)(x,y)))\phi_0(y))\mathrm{d}S_y=\frac{1}{2}\phi_4(x).
\end{aligned}
\tag{76}
$$

The formulations (1), (2), (3), (4) are respectively named u, θ, m, v in [6] where the series expansion of the kernels in polar coordinates can be found. The formulations 1, 2, 3 can also be found in [9] for $\nu=1$.

Appendix B: Proof of the asymptotic expression of the integral over Γ_R

We first give the asymptotic behaviour of $\frac{\partial f}{\partial n}$, $M(f)$, $N(f)$ on Γ_R. We recall the asymptotic behaviour required in (13):

$$
\begin{aligned}
f=\;&A_0r^2\ln(r)-(A_1\cos(\theta)+A_2\sin(\theta))r(2\ln(r)+1)+A_3(\ln(r)+1)\\
&-B_0-B_1r\cos(\theta)-B_2r\sin(\theta)-B_3r^2+c_1\cos(2\theta)+c_2\sin(2\theta)+O\left(\frac{1}{r}\right).
\end{aligned}
\tag{77}
$$

Then we deduce the asymptotic behaviour of $\frac{\partial f}{\partial r}$, $M(f)$, $N(f)$:

$$
\begin{aligned}
\frac{\partial f}{\partial r}=\;&A_0r(2\ln(r)+1)-(A_1\cos(\theta)+A_2\sin(\theta))(2\ln(r)+3)\\
&+A_3/r-B_1\cos(\theta)-B_2\sin(\theta)-2B_3r+O\left(\frac{1}{r^2}\right);
\end{aligned}
\tag{78}
$$

$$
\begin{aligned}
M(f)=\;&A_0(2\nu\ln(r)+2\ln(r)+\nu+3)-\frac{2(\nu+1)}{r}(A_1\cos(\theta)+A_2\sin(\theta))\\
&+\frac{(\nu-1)}{r^2}A_3-2(\nu+1)B_3-\frac{4\nu}{r^2}(c_1\cos(2\theta)+c_2\sin(2\theta)+O\left(\frac{1}{r^3}\right);
\end{aligned}
\tag{79}
$$

$$
N(f)=-\frac{4}{r}A_0-\frac{4}{r^2}(A_1\cos(\theta)+A_2\sin(\theta))
$$

$$-\frac{(1-\nu)}{r^2}(A_1\cos(\theta)+A_2\sin(\theta))(2\ln(r)+3)$$
$$-\frac{(1-\nu)}{r^2}(B_1\cos(\theta)+B_2\sin(\theta))+\frac{8}{r^3}(c_1\cos(2\theta)+c_2\sin(2\theta)+O\left(\frac{1}{r^4}\right). \tag{80}$$

We can now evaluate the limit L of $\int_{\Gamma_R} fN(f^*)+\frac{\partial f}{\partial n}M(f^*)-f^*N(f)-\frac{\partial f^*}{\partial n}M(f)$ when $R\to\infty$. It is found that:

$$L=-8\pi\left(A_0B_0^*+A_1B_1^*+A_2B_2^*+A_3B_3^*-B_0A_0^*-B_1A_1^*-B_2A_2^*-B_3A_3^*\right). \tag{81}$$

For $E(x,y)=\frac{1}{8\pi}|x-y|^2\ln|x-y|$, we have the following asymptotic behaviour when $x\to\infty$ see [18]: $E(x,y))=|x|^2\ln(|x|)-(x_1y_1+x_2y_2)(2\ln(|x|)+1)+(y_1^2+y_2^2)(\ln(|x|+1)+\cos(2\theta)(x_1^2-x_2^2)/2+\sin(2\theta)x_1x_2+O(r^{-1})$. with $y_1=\cos(\theta)|y|$, $y_2=\sin(\theta)|y|$. This means that we have in that particular case:

$$\begin{aligned}&A_0^*=1/8\pi,\quad A_1^*=(1/8\pi)x_1,\quad A_2^*=(1/8\pi)x_2,\\&A_3^*=(1/8\pi)\left(x_1^2+x_2^2\right),\quad B_0^*=0,\quad B_1^*=0,\quad B_2^*=0,\quad B_3^*=0.\end{aligned} \tag{82}$$

Then, substituting (82) in (81), we finally find (15).

Appendix C: Details of matrix elements used in BEM

Taking into account the interpolation functions described in Sect. 7, the matrix elements of each matrix are described below.

– Matrix $\left[A'\right]$

$$A'_{ij}=\frac{1}{2}r^2\ln r^2, \tag{83}$$
$$A'_{ii}=0, \tag{84}$$

where $r=\left\|\mathbf{z}_i-\mathbf{z}_j\right\|$.

– Matrix $\left[B'\right]$

$$\begin{aligned}B'_{ij}&=B'(\mathbf{z}_i,\mathbf{x}_j)\\&=\int_{e_j}\frac{\partial E_0}{\partial n_y}(\mathbf{x}_i,\mathbf{y})\mathrm{d}S_y=a\int_{h_1}^{h_2}(\ln(a^2+h^2)+1)\mathrm{d}h=a\left[J_0(h)+h\right]_{h_1}^{h_2},\end{aligned} \tag{85}$$

where

$$h=(\mathbf{y}-\mathbf{x}_i).\mathbf{t}, \tag{86}$$
$$a=(\mathbf{y}-\mathbf{x}_i).\mathbf{n}, \tag{87}$$
$$J_0(h)=h.\ln(a^2+h^2)-2h+2a.\arctan\frac{h}{a}, \tag{88}$$

h_1 and h_2 are computed at each end point of the element e_j.

– Matrix $[C]$

$$C_{ij}=-2(\ln r+1)y_{n_x}, \tag{89}$$

with

$$r=\left\|\mathbf{x}_i-\mathbf{z}_j\right\|, \tag{90}$$
$$y_{n_x}=(\mathbf{z}_j-\mathbf{x}_i).\mathbf{n}_x(\mathbf{x}_i), \tag{91}$$

where $\mathbf{n}_x(\mathbf{x}_i)$ is the unit normal to the element containing $\mathbf{x}_i$.

– Matrix $[D]$

$$D_{ij} = D(\mathbf{x}_i, \mathbf{x}_j) = \int_{e_j} \frac{\partial^2 E_0}{\partial n_x \partial n_y} \mathrm{d}S_y = \left[-2\alpha a J_3 - 2a\beta J_4 - \alpha(J_0 + h)\right]_{h_1}^{h_2}, \tag{92}$$

where

$$\alpha = \mathbf{n}.\mathbf{n}_x, \tag{93}$$
$$\beta = \mathbf{t}.\mathbf{n}_x, \tag{94}$$
$$J_3 = \int \frac{a\mathrm{d}h}{a^2 + h^2} = \left[\arctan\left(\frac{x}{a}\right)\right], \tag{95}$$
$$J_4 = \int \frac{h\mathrm{d}h}{a^2 + h^2} = \frac{1}{2}\left[\ln(a^2 + h^2)\right]. \tag{96}$$

When $a = 0$, these terms become:

$$D_{ij} = -\alpha \int (2\ln h + 1)\mathrm{d}h = -\alpha h \left[\ln h^2 - 1\right]_{h_1}^{h_2}. \tag{97}$$

For singular matrix elements, there is also $\alpha = 1$, and

$$D_{ii} = -h\left[\ln h^2 - 1\right]_{-l/2}^{l/2}. \tag{98}$$

where l is the length of the element.

– Matrix $[G]$

$$G_{il} = -q_l(\mathbf{z}_i), \tag{99}$$

where q_l are the polynomial functions defined in subsection 7.1.

– Matrix $[H]$

$$[H]_i = -\left[0,\ n_1(\mathbf{x}_i),\ n_2(\mathbf{x}_i),\ 2\mathbf{x}_i.\mathbf{n}\,(\mathbf{x}_i)\right]. \tag{100}$$

– Matrix $[E]$

$$E_{lj} = q_l(\mathbf{z}_j). \tag{101}$$

– Matrix $[F]$

$$\left[F_j\right] = \begin{bmatrix} 0 \\ l_j n_1(\mathbf{x}_j) \\ l_j n_2(\mathbf{x}_j) \\ 2l_j \mathbf{n}(\mathbf{x}_j).\mathbf{x}_j \end{bmatrix}. \tag{102}$$

References

1. Ambartsumian, S.A.: The theory of transverse bending of plates with asymmetric elasticity. Mech. Compos. Mater. **32**(1), 583–596 (2004)
2. Bézine, G.: Boundary integral formulation for plate flexure with arbitrary boundary conditions. Mech. Res. Commun. **5**(4), 197–206 (1978)
3. Chapko, R., Johansson, B.T.: An iterative regularizing method for an incomplete boundary data problem for the biharmonic equation. Z. Angew. Math. Mech. **98**, 2010–2021 (2018)
4. Chen, J.T., Chou, K.S., Hsieh, C.C.: Derivation of stiffness and flexibility for rods and beams by using dual integral equations. Eng. Anal. Bound. Elem. **32**, 108–121 (2008)
5. Chen, J.T., Kuo, S.R., Chang, Y.L., Kao, S.K.: Degenerate-scale problem of the boundary integral equation method/boundary element method for the bending plate analysis. Eng. Comput. **34**(5), 1527–1550 (2017)
6. Chen, J.T., Wu, C.S., Chen, K.H., Lee, Y.T.: Degenerate scale for the analysis of circular thin plate using the boundary integral equation method and boundary element methods. Comput. Mech. **38**(1), 33–49 (2006)
7. Chen, Y.Z., Lin, X.Y., Wang, Z.X.: Evaluation of the degenerate scale for BIE in plane elasticity by using conformal mapping. Eng. Anal. Bound. Elem. **33**, 147–158 (2009)

8. Chen, Y.Z., Wang, Z.X., Lin, X.Y.: The degenerate scale problem for the Laplace equation and plane elasticity in a multiply connected region with an outer circular boundary. Int. J. Solids Struct. **46**, 2605–2610 (2009)
9. Christiansen, S.: Derivation and analytical investigation of three direct boundary integral equations for the fundamental biharmonic problem. J. Comput. Appl. Math. **91**(2), 231–247 (1998)
10. Christiansen, S.: On the elastostatic significance of four boundary integrals involving biharmonic functions. Acta Mech. **126**, 37–43 (1998)
11. Christiansen, S.: Detecting non-uniqueness of solutions to biharmonic integral equations through SVD. J. Comput. Appl. Math. **134**(1–2), 23–35 (2001)
12. Constanda, C.: A Mathematical Analysis of Plates with Transverse Shear Deformation. Longman Scientific & Technical, Harlow (1990)
13. Constanda, C.: On the Dirichlet Problem for the Two-dimensional Biharmonic Equation. Math. Methods Appl. Sci. **20**(10), 885–890 (1997)
14. Corfdir, A., Bonnet, G.: Variational formulation and upper bounds for degenerate scales in plane elasticity. J. Elast. **118**(2), 209–221 (2015)
15. Corfdir, A., Bonnet, G.: Exact degenerate scales in plane elasticity using complex variable methods. Int. J. Solids Struct. **80**, 430–444 (2016)
16. Corfdir, A., Bonnet, G.: The degenerate scales for plane elasticity problems in piecewise homogeneous media under general boundary conditions. J. Elast. **140**, 49–77 (2020). https://doi.org/10.1007/s10659-019-09757-5
17. Costabel, M.: The biharmonic double layer potential in Lipschtiz domains. Workshop, Linz University (2006). https://perso.univ-rennes1.fr/martin.costabel/publis/Linz_DblBih.pdf
18. Costabel, M., Dauge, M.: Invertibility of the biharmonic single layer potential operator. Integral Eqn. Oper. Theory **24**(1), 46–67 (1996)
19. Costabel, M., Dauge, M.: Solvability of a system of integral equations for clamped plates. In: Morino, L., Wendland, W.L. (eds.) IABEM Symposium on Boundary Integral Methods for Nonlinear Problems, pp. 41–46. Springer, Dordrecht (1997)
20. Costabel, M., Lusikka, I., Saranen, J.: Comparison of three boundary elements approaches for the solution of the clamped plate problem. In: C.A. Brebbia, W.L. Wendland, G. Kuhn (eds.) Boundary Elements IX, Vol. 2: Stress Analysis Applications, pp. 19–34. Springer Verlag, Berlin (1987)
21. Fuglede, B.: On a direct method of integral equations for solving the biharmonic Dirichlet problem. Z. Angew. Math. Mech. **61**, 449–459 (1981)
22. Goursat, E.: Sur l'équation $\Delta\Delta u = 0$ (On biharmonic equation). Bull. Soc. Math. France **26**, 236–237 (1898)
23. Hadamard, J.: Mémoire sur le problème d'analyse relatif à l'équilibre des plaques élastiques encastrées (Dissertation on a problem related to the equilibrium of clamped elastic plates). Mémoires présentés par divers savants à l'Académie des Sciences **33**, 1–128 (1908)
24. Hayes, J., Kellner, R.: The eigenvalue problem for a pair of coupled integral equations arising in the numerical solution of Laplace's equation. SIAM J. Appl. Math. **22**(3), 503–513 (1972)
25. He, W.J.: An equivalent boundary integral formulation for bending problems of thin plates. Comput. Struct. **74**, 319–322 (2000)
26. Hsiao, G.C.: On the stability of integral equations of the first kind with logarithmic kernels. Arch. Ration. Mech. Anal. **94**(2), 179–192 (1986)
27. Hsiao, G.C., Kleinmann, R.E.: On a uniform characterization of capacity. In: Král, J. (ed.) Potential Theory, pp. 103–126. Plenum Press, Prague (1987)
28. Hsiao, G.C., Steinbach, O., Wendland, W.L.: Domain decomposition methods via boundary integral equations. J. Comput. Appl. Math. **125**, 521–537 (2000)
29. Hsiao, G.C., Wendland, W.L.: A characterization of the Calderón projector for the biharmonic equation. In: Begher, H.G.W., Nicolosi, F. (eds.) More Progresses in Analysis, Proceedings of the 5th international ISAAC Congress, pp. 23–38. World Scientific Publishing (2005)
30. Hsiao, G.C., Wendland, W.L.: Boundary integral equations. In: Applied Mathematical Sciences, vol. 164. Springer, Berlin (2008)
31. Jaswon, M.: Numerical biharmonic analysis and some applications. Int. J. Solids Struct. **3**(3), 309–332 (1967)
32. Jaswon, M.A., Maiti, M.: An integral equation formulation of plate bending problems. J. Eng. Math. **2**(1), 83–93 (1968)
33. Karachik, V.V., Sadybekov, M., Torebek, B.T.: Uniqueness of solutions to boundary-value problem for the biharmonic equation in a ball. Electron. J. Differ. Equ. **2015**(244), 1–9 (2015)
34. Lauricella, G.: Sur l'intégration de l'équation relative à l'équilibre des plaques élastiques encastrées (On the integration of the equation related to the equilibrium of clamped elastic plates). Acta Math. **32**, 201–256 (1909)
35. Meleshko, V., Selvadurai, A.: Contributions to the theory of elasticity by louis napoleon george filon as viewed in the light of subsequent developments in biharmonic problems in applied mechanics and engineering mathematics. J. Eng. Math. **46**(3–4), 191–212 (2003)
36. Meleshko, V.V.: Selected topics in the history of the two-dimensional biharmonic problem. Appl. Mech. Rev. **56**(1), 33–85 (2003)
37. Mikhlin, S.: Integral Equations and their Application to Certain Problems in Mechanics, Physics and Technology. Pergamon Press, Oxford (1957)
38. Mindlin, R.D.: Influence of rotary inertia and shear on flexural motions of isotropic, elastic plates. ASME J. Appl. Mech. **18**, 31–38 (1951)
39. Mitra, A.K., Das, S.: Nonuniqueness in the integral equation formulation of the biharmonic equation in multiply connected domains. Comput. Methods Appl. Mech. Eng. **69**(2), 205–214 (1988). https://doi.org/10.1016/0045-7825(88)90188-0
40. Mitrea, I., Mitrea, M.: Multi-layer potentials and boundary value problems. In: Lecture Notes in Mathematics. Springer, Heidelberg (2013)
41. Muskhelishvili, N.: Sur la solution du problème biharmonique pour l'aire extérieure à une ellipse (On the solution fo the biharmonic problem for the domain exterior to an ellipse). Math. Z. **26**, 700–705 (1927)

42. Muskhelishvili, N.I.: Applications des intégrales analogues à celles de Cauchy à des problèmes de la physique mathématique (Application of integrals analogous to Cauchy integrals to some problems of mathematical physics). Université de Tiffliz, Tiffliz (1922)
43. Muskhelishvili, N.I.: Singular Integral Equations. Noordhoff, Gronningen (1953)
44. Muskhelishvili, N.I.: Some Basic Problems of the Mathematical Theory of Elasticity. Noordhoff, Gronningen (1953)
45. Ogawa, S., Yotsuya, I.: Some radii associated with polyharmonic equation, II. Proc. Jpn. Acad. **47**(4), 368–373 (1971). https://doi.org/10.3792/pja/1195519970
46. Pólia, G., Szegö, G.: Isoperimetric inequalities in mathematical physics. In: No. 27 in Annals of Mathematic Studies. Princeton University Press, Princeton (1951)
47. Reddy, J.: A generalization of two-dimensional theories of laminated composite plates. Commun. Appl. Numer. Methods **3**, 173–180 (1987)
48. Reissner, E.: The effect of transverse shear deformation on the bending of elastic plates. ASME J. Appl. Mech. **12**, 69–77 (1945)
49. Rogers, T., Watson, P., Spencer, A.: Exact 3-dimensional elasticity solutions for bending of moderately thick inhomogeneous and laminated strips under normal-pressure. Int. J. Solids Struct. **32**(12), 1659–1673 (1995)
50. Selvadurai, A.P.S.: Partial differential equations in mechanics-2. In: Biharmonic Equation, Poisson's Equation. Springer, Berlin (2000)
51. Shigeta, T., Young, D.L.: Regularized solutions with a singular point for the inverse biharmonic boundary value problem by the methods of fundamental solutions. Eng. Anal. Bound. Elem. **35**, 883–894 (2011)
52. Soldatos, K.P.: A transverse shear deformation theory for homogeneous monoclinic plates. Acta Mech. **94**, 195–220 (1992)
53. Vodička, R.: An asymptotic property of degenerate scales for multiple holes in plane elasticity. Appl. Math. Comput. **220**, 166–175 (2013)
54. Vodička, R., Mantič, V.: On invertibility of elastic single-layer potential operator. J. Elast. **74**(2), 147–173 (2004)
55. Wang, W.: N-capacity, n-harmonic radius and n-harmonic transplantation. J. Math. Anal. Appl. **327**, 155–174 (2007)